

Design-Based Inference for Spatial Experiments under Unknown Interference

Ye Wang, Cyrus Samii, Haoge Chang, and P. M. Aronow*

March 13, 2023

*Wang is Assistant Professor, Department of Political Science, University of North Carolina, Chapel Hill, (Email: yewang@unc.edu). Samii (contact author) is Associate Professor, Department of Politics, New York University (Email: cds2083@nyu.edu). Chang is PhD. Candidate, Department of Economics, Yale University (Email: haoge.chang@yale.edu). Aronow is Associate Professor, Departments of Political Science and Biostatistics, Yale University (Email: p.aronow@yale.edu). For their comments and suggestions, we thank Kirill Borusyak, Stephen Cole, Alexander Demin, Naoki Egami, Jiawei Fu, Michael Hudgens, Peter Hull, Molly Roberts, Fredrik Sävje, Davide Viviano, and seminar participants at Harris School at University of Chicago, New York University Abu Dhabi, Princeton University, Rochester University, Texas A&M., UNC, and UCSD

Design-Based Inference for Spatial Experiments under Unknown Interference

Abstract

We consider design-based causal inference in settings where randomized treatments have effects that bleed out into space in complex ways that overlap and in violation of the standard “no interference” assumption for many causal inference methods. We define a spatial “average marginalized effect,” which characterizes how, in expectation, units of observation that are a specified distance from an intervention node are affected by treatment at that node, averaging over effects emanating from other intervention nodes. We establish conditions for non-parametric identification under unknown interference, asymptotic distributions of estimators, and recovery of structural effects. We propose methods for both sample-theoretic and permutation-based inference. We provide illustrations using randomized field experiments on forest conservation and health. **Keywords:** causal inference, design-based inference, experiments, interference, spatial statistics.

1 Introduction

Consider an experiment where an intervention is randomly assigned to specific points or polygons in a geographic space. Then, we observe how outcomes are distributed over this geography. Figure 1 illustrates the generic structure of such experiments. The left panel presents a potential point-intervention experiment. The points are locations at which an intervention might be applied. An experimental design could treat half of such points to receive the intervention (gray shaded points), with the rest of the points remaining in a control condition without intervention (unshaded points). The shading in the background raster indicates outcome values. The right panel illustrates a similar situation, but with interventions assigned to polygons instead of points.

For point interventions, a standard way to analyze such experiments is to, first, define the units of observation as the areas in the immediate vicinity of points of intervention, and then the treatment status of the intervention point defines the treatment status of the areal unit. For polygon interventions, the polygons themselves are the units of observation. Then, the difference in average outcomes across treated versus control units is taken to be an estimate of the average treatment effect (ATE). A key identifying assumption is that potential outcomes for a given unit depend only on the treatment status of that unit (e.g., the nearest site of intervention in the case of point interventions) (Imbens and Rubin, 2015, p. 10). A recent example is Jayachandran et al. (2017), who study a forest conservation experiment by comparing forest cover outcomes in and around villages that hosted a conservation intervention to those that did not.

The problem is that this difference in means does not equal the ATE when the effect of intervening at a given point or polygon bleeds out into other areas since potential outcomes depend not only on a unit's own treatment status (Halloran and Struchiner, 1995). It is often reasonable to expect such spill-over effects. Incentives provided by a forest conservation

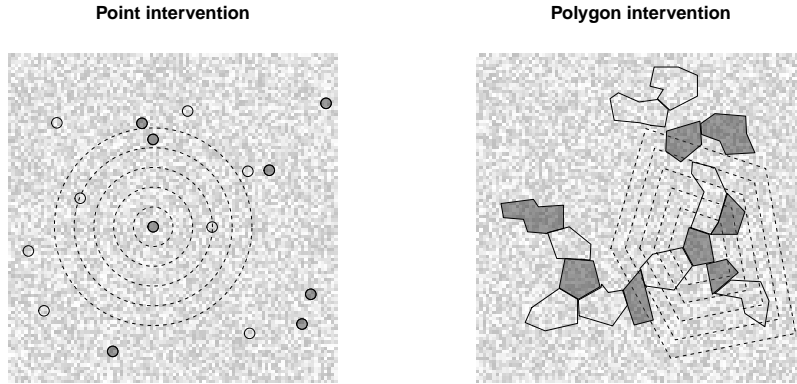


Figure 1: Illustrations of hypothetical spatial experiments in which interventions are applied to points (left) or polygons (right). The background raster captures the geographic outcome data. We allow for the possibility for effects to bleed out in space, as illustrated by the concentric dashed lines.

intervention may motivate villagers to displace deforestation, causing it to decrease near the boundary of the villages, but then to increase further away. The displacement effect from one village may interact with the effect from another village, making the overall effects complex. We can imagine similarly complex spatial effects from other types of interventions. Vaccination campaigns can have spatial effects on disease prevalence through herd immunity. Product campaigns can have spatial effects on consumer behavior by word-of-mouth or strategic responses of other firms. The dashed lines in Figure 1 display possible zones into which effects may bleed out in our hypothetical examples. Such spatial effects are instances of “interference,” whereby a unit’s potential outcomes depend not only on that unit’s treatment status but rather on the overall distribution of treatments (Cox, 1958, p. 19).

This paper develops design-based methods for accounting for such interference in analyzing spatial experiments. Design-based methods derive causal and statistical inferential properties from the experimental design, which is typically under the control of the analyst. We show that when interference is present, rather than estimating the ATE, contrasts between treated and control areas capture a more nuanced, but nonetheless, policy-relevant

quantity that we call the “average marginalized effect” (AME).¹ We can define AMEs at different distance intervals from where the intervention is applied. The AME is similar to the average direct effect of [Halloran and Struchiner \(1995\)](#) (see also [Hudgens and Halloran \(2008\)](#), [VanderWeele and Tchetgen \(2011\)](#), [Sävje et al. \(2021\)](#), [Li and Wager \(2022\)](#), and [Hu et al. \(2022\)](#)), except that it is indexed by distance for application to the spatial case. The AME measures how, on average, outcomes within the specified distance interval from an intervention node are affected by activating a treatment at that node, taking into account ambient effects emanating from treatments at other intervention nodes. There is a direct mapping from the AME to the types of effects that are assumed by parametric models of spatial effects: when effects emanating from different intervention nodes are additive, the AME recovers the average of these additive effects. If spatial effects are not simply additive but exhibit complex interactions, the AME still yields an interpretable and policy-relevant quantity.

Inference also needs to account for the dependencies that interference creates. We work with a Horvitz-Thompson estimator, a Hajek estimator, and a kernel regression estimator for the AME. We show that these estimators are consistent and asymptotically normal under weak restrictions on the degree of interdependence induced by interference. We further prove that the commonly-used spatial heteroscedasticity and autocorrelation consistent (HAC) variance estimator of [Conley \(1999\)](#) provides conservative estimates for the true variance of these estimators under conditions that are often satisfied in practice.

Our analysis is related to a few streams of current methodological research. First, our approach draws most directly on recent design-based analyses of causal effects under interference that consider estimands marginalized over the randomization distribution, as in [Hudgens and Halloran \(2008\)](#), [Sävje et al. \(2021\)](#), [Papadogeorgou et al. \(2020\)](#), [Li and Wager](#)

¹Previous versions of this paper used “average marginalized response,” but we revised the terminology since “response” is often used in the literature to refer to potential outcomes, rather than effects.

(2022), and [Hu et al. \(2022\)](#). As in these approaches, our inference does not require that we specify the precise structure of the interference network (i.e., the “exposure mapping”, following [Aronow and Samii \(2017\)](#)). It also skirts the issue of non-overlap caused by defining the estimand using the potentially high-dimensional treatment exposure ([Leung, 2022b](#)). Second, our analysis is related to recent work on non-parametric estimation of spatial effects, including work on “bipartite causal inference” by [Zigler and Papadogeorgou \(2018\)](#) and on cluster-randomized designs by [Leung \(2022b\)](#). These works focus on cases where points of intervention are far enough apart to yield disjoint clusters that interfere with each other minimally. Such designs are appealing, but they are not always feasible. Similar to m -dependence for a time series, we assume hard limits on the extent of interference, but we do not assume that the set of units can be partitioned into a set of disjoint clusters with tractable interference-induced dependencies between any of them. Third, our inferential results rely on the contributions of [Ogburn et al. \(2020\)](#). We also draw connections to inferential results in the spatial econometrics literature ([Arbia, 2006](#); [Jenish, 2016](#); [Kelejian and Piras, 2017](#)). We justify the usage of regression estimators in the spatial setting from the design-based perspective and provide causal interpretations for the coefficients. We clarify the connection to [Conley \(1999\)](#)’s spatial HAC variance estimator.

We begin by developing the formal inferential setting and main theoretical results, using a simple toy example to illustrate concepts. We then develop a number of extensions and refinements. We provide simulation evidence of the performance of our proposed estimators and then turn to applications based on experiments in public health and forest conservation.

2 Setting

Suppose a set of intervention nodes $\mathcal{N} = \{1, \dots, N\}$. Each node $i \in \mathcal{N}$ can be either a point or a collection of points (e.g., a polygon) that resides in a two-dimensional set \mathcal{X} indexed by

$x = (x_1, x_2)$ (e.g., latitude and longitude). An experimental design assigns a binary treatment $Z_i \in \{0, 1\}$ to each intervention node. The ordered vector of experimental assignment variables is $\mathbf{Z} \equiv (Z_1, \dots, Z_N)$, and the *ex post* realized assignment from the experiment is given by $\mathbf{z} \equiv (z_1, \dots, z_N)$. The experimental design fixes the set of possible assignment vectors \mathcal{Z} as well as a probability distribution over that set, $\mathbb{P}_{\mathbf{z}}$. Our analysis below considers the case of an experimental design based on Bernoulli randomization for each Z_i —i.e., (possibly weighted) coin flips to determine treatment status at each node. Analogous to the relationship between sampling with and without replacement, Bernoulli assignment is also a reasonable, if typically conservative, inferential approximation for completely randomized designs when N is large. We discuss other differences between Bernoulli and completely randomized designs below.

Potential outcomes at any point $x \in \mathcal{X}$ are defined for each value of \mathbf{z} , $(Y_x(\mathbf{z}))_{\mathbf{z} \in \mathcal{Z}}$. Given a realized treatment assignment, \mathbf{z} , we observe the corresponding potential outcome at x :

$$Y_x = \sum_{\mathbf{z} \in \mathcal{Z}} Y_x(\mathbf{z}) I(\mathbf{Z} = \mathbf{z}).$$

Data for points in \mathcal{X} may come in various formats including raster data or data for a discrete set of points in \mathcal{X} . Let $\mathbf{Y}(\mathbf{z}) = (Y_x(\mathbf{z}))_{x \in \mathcal{X}}$ denote the full set of potential outcomes when $\mathbf{Z} = \mathbf{z}$ and $\mathbf{Y} = (Y_x(\mathbf{Z}))_{x \in \mathcal{X}}$ denote the full set of realized outcomes.

We map the full set of potential outcomes $\mathbf{Y}(\mathbf{z})$ for all points in the outcome space \mathcal{X} back to the intervention nodes in \mathcal{N} by defining the “circle average” function:

$$\mu_i(\mathbf{Y}(\mathbf{z}); \Omega_d) = \frac{1}{|\{x : d_i(x) \in \Omega_d\}|} \int_{x: d_i(x) \in \Omega_d} Y_x(\mathbf{z}) d\zeta.$$

In the expression above, $d_i(x)$ measures the distance between point x and intervention node i . When i is a point located at $x(i)$, $d_i(x) = \|x(i) - x\|$, where $\|\cdot\|$ is some well-defined metric (e.g., Euclidean or a least-cost distance). If i is a collection of points, then $d_i(x) =$

$\min_{x' \in i} \|x' - x\|$, the minimal distance between x and points belonging to i . Ω_d is a set of distance values and ζ is a suitable measure on \mathcal{X} . Therefore, $\mu_i(\mathbf{Y}(\mathbf{z}); \Omega_d)$ is the average outcome across points whose distance to i falls in Ω_d . If the points in \mathcal{X} are dense and spaced evenly, then Ω_d could be a singleton: $\{d_i(x) : d_i(x) = d\}$. The circle average amounts to taking the average across points along the edge of a circle of radius d around i . If the points are spaced such that there are few or no points precisely at the edge of the circle, Ω_d could be a “donut,” $\{d_i(x) : d - \kappa < d_i(x) \leq d\}$,² or a “disk,” $\{d_i(x) : d_i(x) \leq d\}$. By considering a collection of disjoint sets, $\{\Omega_d\}_{d \in \mathcal{D}}$, we will be able to examine how the circle average’s value varies over the geography.³ When it does not cause confusion, we write $\mu_i(\mathbf{Y}(\mathbf{z}); \Omega_d)$ simply as $\mu_i(\mathbf{Y}(\mathbf{z}); d)$. Similarly, the realized circle average for intervention node i at d is

$$\mu_i(\mathbf{Y}; d) = \sum_{\mathbf{z} \in \mathcal{Z}} \mu_i(\mathbf{Y}(\mathbf{z}); d) I(\mathbf{Z} = \mathbf{z}).$$

This representation allows us to see how an experiment is a process of sampling potential circle averages for intervention nodes, and therefore allows us to apply sample theoretic (in particular, Horvitz-Thompson- and Hajek-type) results in our analysis below.

The left plot in Figure 2 illustrates a toy example with a point intervention ($N = 4$) and raster outcome data. The plot shows a “null raster” for which none of the intervention nodes has been assigned to treatment and so $\mathbf{z} = (0, 0, 0, 0)$, in which case outcomes are $Y_x(0, 0, 0, 0)$ for all x in the space. As we can see, outcomes are defined for any point x in the space, although outcomes are constant within raster cells. This is a feature of raster data. Other types of data may exhibit finer levels of granularity — e.g., data produced from kriging interpolation that varies smoothly in space. We take these outcome data, and any coarsening

² κ is a user-chosen constant that dictates the donut’s thickness.

³Note that we do not require the union of $\{\Omega_d\}_{d \in \mathcal{D}}$ to be the entire geography although we do not exclude this possibility either.

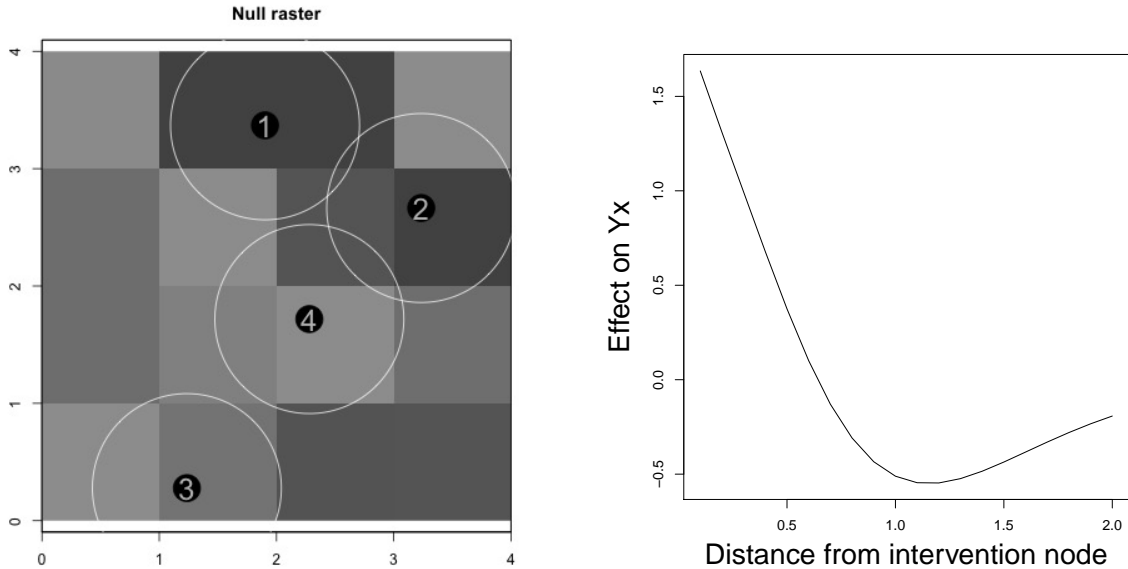


Figure 2: Left: Illustration of a “null raster,” with $N = 4$ intervention nodes (points), none of which are assigned to treatment. The coloring of the raster cells corresponds to outcome levels. White circles around the nodes are circle averages based on the Euclidean distance. Right: Illustration of a possible effect function such that treatments transmit effects non-monotonically in distance. When multiple intervention nodes are treated, these effects accumulate.

or smoothing operations that they incorporate, as fixed. For our design-based inference, the only source of stochastic variation is from \mathbf{Z} .⁴ White circles around the intervention nodes demonstrate one possible way to construct the circle average. We use the Euclidean distance and take averages across all the raster cells passed by the edge of the circles. Note that we do not prohibit circles around different nodes to intersect with each other.

As discussed above, spatial effects can exhibit considerable complexity. For the sake of illustration, suppose in our toy example that treatments tend to transmit effects that are non-monotonic in distance and that these effects simply accumulate in an additive manner. The right plot in Figure 2 illustrates such an effect function. Then, the net result would depend on how treatments are distributed over the intervention points. Figure 3 illustrates

⁴For data that are smoothed using kriging, we would tune smoothing parameters on auxiliary data so that they are fixed with respect to \mathbf{Z} .

how outcomes would be affected over different allocations of the treatment given that effects take the form as in Figure 2. We emphasize that in the analysis below, we do not assume that effects are additive or homogenous in form—this is done here merely to provide a simple illustration.

3 Defining a marginal spatial effect

As the potential outcome notation for $Y_x(\mathbf{z})$ indicates, the outcome at any point may depend on the full vector of realized treatment assignments, \mathbf{z} . Similarly, the potential outcome notation for the circle average, $\mu_i(\mathbf{Y}(\mathbf{z}); d)$, suggests that the realized circle average for node i may depend on treatment assignments for nodes other than i . As such, the circle averages are potentially subject to causal interference.

We now define a spatial effect that we call the “average marginalized effect” (AME). The AME accounts for interference. It is a marginal effect (Rubin, 2005) that bears resemblance to the “average direct effect” of Halloran and Struchiner (1995) and the “average direct causal effect” defined by Hudgens and Halloran (2008) and is a spatial analogue of the “expected average treatment effect” defined by Sävje et al. (2021) or the “average indirect effect” in Hu et al. (2022). The usual definition of a unit-level treatment effect takes the difference between a unit’s potential outcomes under one treatment condition versus under another treatment condition. A unit-level marginal effect is different because it takes the difference between the average of a unit’s potential outcomes over a set of potential outcomes versus the average over another set. We apply this idea to the spatial setting. In doing so, we consider effects that may bleed out in ways that are not necessarily contained within pre-defined strata, as in Hudgens and Halloran (2008).

To define the spatial AME, first rewrite the potential outcome at point x as $Y_x(z_i, \mathbf{z}_{-i})$, where \mathbf{z}_{-i} is a vector equalling \mathbf{z} except that the value for intervention node i is omitted. This

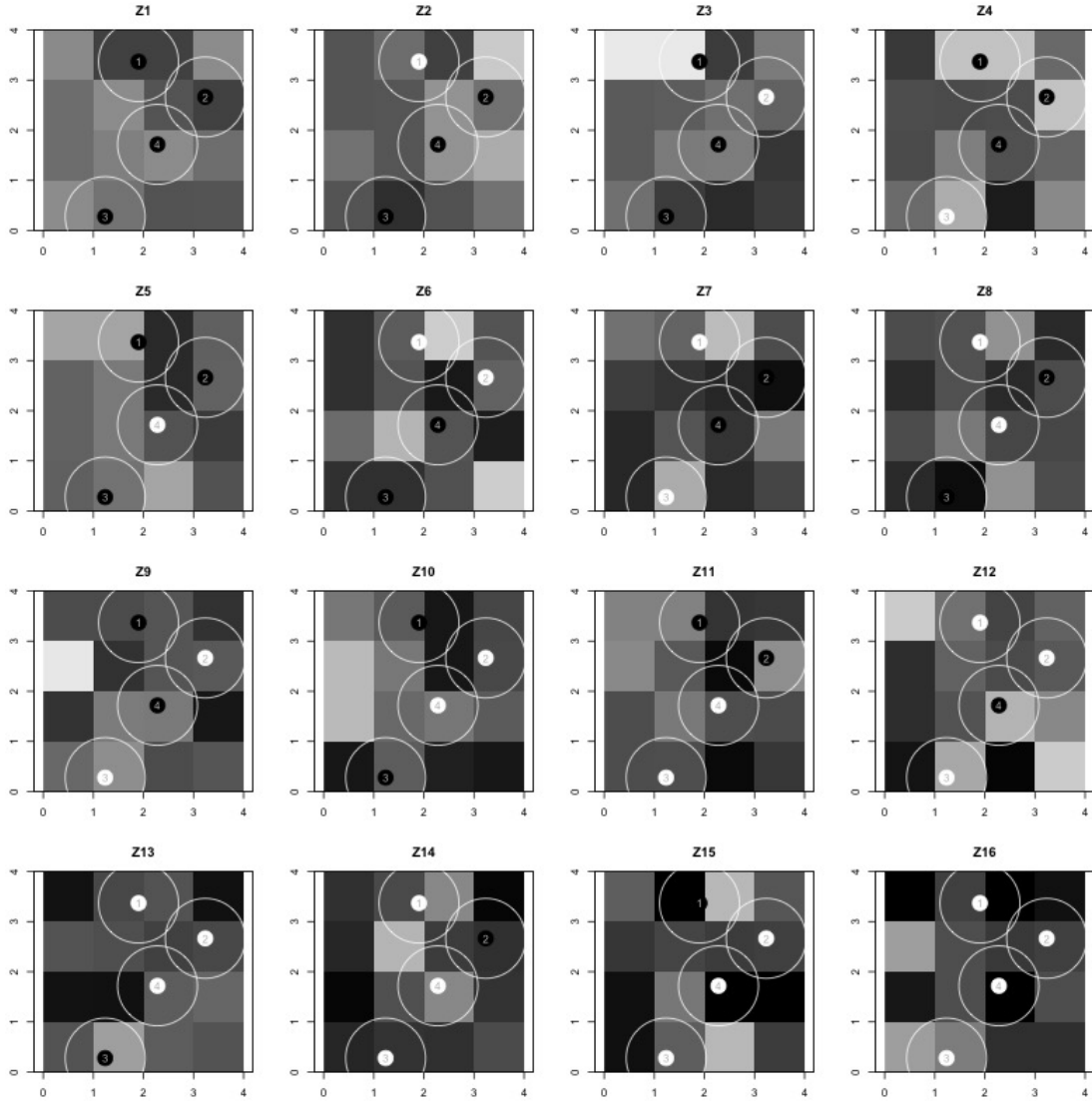


Figure 3: Illustration of how outcomes are affected given different allocations of treatment and effects that take the form as presented in the right plot of Figure 2. Treated intervention points are white, while non-treated intervention points are black.

allows us to pay special attention to how variation in treatment at node i relates to potential outcomes at point x , given the variation in treatment values in \mathbf{z}_{-i} . We can marginalize over variation in \mathbf{z}_{-i} to define an “individualistic” average of potential outcomes for point x , holding the treatment at intervention node i to treatment value z :

$$Y_{ix}(z; \eta) = \mathbb{E}_{\mathbf{z}_{-i}}[Y_x(z, \mathbf{Z}_{-i})] = \sum_{\mathbf{z}_{-i} \in \mathcal{Z}_{-i}} Y_x(z, \mathbf{z}_{-i}) \Pr(\mathbf{Z}_{-i} = \mathbf{z}_{-i}; \eta),$$

where η is the experimental design parameter that governs the distribution of \mathbf{Z} (that is, the probability of treatment assignments) and \mathcal{Z}_{-i} is the set of possible values that \mathbf{Z}_{-i} can take. This is the individualistic marginal potential outcome at point x given that node i is assigned to treatment condition z , marginalizing over possible assignments to other nodes. We can use Figure 3 to illustrate. To construct $Y_{1x}(0; \eta)$, one would take a weighted average of the potential outcomes at point x under assignments labeled in the figure as Z1, Z3, Z4, Z5, Z9, Z10, Z11, and Z15, where the weights would be proportional to the probability of each assignment.

We can define a similar marginal quantity at the level of the circle averages:

$$\mu_i(z; d, \eta) = \mathbb{E}_{\mathbf{z}_{-i}}[\mu_i(\mathbf{Y}(z, \mathbf{Z}_{-i}); d)] = \sum_{\mathbf{z}_{-i} \in \mathcal{Z}_{-i}} \mu_i(\mathbf{Y}(z, \mathbf{z}_{-i}); d) \Pr(\mathbf{Z}_{-i} = \mathbf{z}_{-i}; \eta),$$

where we use $\mathbf{Y}(z, \mathbf{z}_{-i})$ to denote the set of potential outcomes over points in \mathcal{X} that obtain under treatment assignment (z, \mathbf{z}_{-i}) . This is the potential circle average at distance d around node i , given that i is assigned to treatment condition z , marginalizing over possible assignments to other nodes. The quantity $\mu_i(z; d, \eta)$ is simply the circle average of the $Y_{ix}(z; \eta)$ values, given that $\Pr(\mathbf{Z}_{-i} = \mathbf{z}_{-i}; \eta)$ is constant over x .

We can now define an *individualistic marginalized effect* at point x of intervening on node

i , allowing other nodes to vary as they otherwise would under η :

$$\tau_{ix}(\eta) = Y_{ix}(1; \eta) - Y_{ix}(0, \eta).$$

This defines the response at point x of switching node i from no treatment to active treatment, averaging over possible treatment assignments to nodes other than i . At the level of circle averages, we can define

$$\tau_i(d; \eta) = \mu_i(1; d, \eta) - \mu_i(0; d, \eta),$$

which is the average of individualistic responses for points along the circle at distance d around node i . Using Figure 3 to illustrate, one would construct $\tau_1(d; \eta)$ by working with the d -radius circle averages around intervention node 1, taking the difference between the mean of the circle averages under assignments Z2, Z6, Z7, Z8, Z12, Z13, Z14, and Z16 minus the mean of circle averages under assignments Z1, Z3, Z4, Z5, Z9, Z10, Z11, and Z15.

Finally, define the *average marginalized effect* (AME) for distance d by taking the mean over the intervention nodes:

$$\tau(d; \eta) = \frac{1}{N} \sum_{i=1}^N \tau_i(d; \eta).$$

The interpretation of the AME for distance d is the average effect of switching a node $i \in \mathcal{N}$ to treatment on points at distance d from that node, marginalized over possible realizations of treatment statuses in other intervention nodes. The distribution of these possible realizations of treatment statuses depends on the experimental design. When $d = 0$, the AME captures the direct effect generated by the treatment at the location of intervention, in a way very similar to the “average direct causal effect” in [Hudgens and Halloran \(2008\)](#) and the “expected average treatment effect” in [Sävje et al. \(2021\)](#).

Our formal analysis focuses on experimental designs that use Bernoulli assignment, in

which case the \mathcal{Z} consists of the 2^N possible vectors that could be obtained from N (possibly differentially weighted) coin flips. This allows for a relatively clean definition of causal effects, as discussed by [Sävje et al. \(2021\)](#) in relation to the expected average treatment effect. This is because Bernoulli assignment ensures that $(1, \mathbf{z}_{-i})$ and $(0, \mathbf{z}_{-i})$ each has positive probability of occurring. In this case, the marginal quantities $Y_{ix}(1; \eta)$ and $Y_{ix}(0; \eta)$ are defined by marginalizing over the same sets of \mathbf{z}_{-i} values, and the individualistic response has a clear *ceteris paribus* interpretation with respect to variation in the treatment assignment at intervention node i . Things are different under complete random assignment, where a fixed number N_1 of nodes are assigned to treatment. Then, for $Y_{ix}(1; \eta)$, one marginalizes over assignments with $N - 1$ units assigned to treatment, while for $Y_{ix}(0; \eta)$, one marginalizes over assignments with N units assigned to treatments. As N grows, these differences between Bernoulli and complete random assignment typically become negligible for the Hajek estimator (discussed below) when interference is local. In those circumstances, at least under the regularity conditions that we propose below, one could consider a design that uses complete random assignment as an approximation to the cleaner Bernoulli case in large samples.

4 Inferential assumptions

In this section, we lay out the assumptions on the experimental design and potential outcomes, including a statement about restrictions on the extent of interference. In the sections that follow, we characterize an unbiased, consistent, and asymptotically normal Horvitz-Thompson estimator for the AME. Then, we characterize a more efficient, consistent, and asymptotically normal Hajek estimator for the AME. Finally, we express the Hajek estimator as a regression estimator and characterize a variance estimator based on the spatial heteroscedasticity and autocorrelation consistent (spatial HAC) estimator of [Conley \(1999\)](#). Thus, our proposed estimator for the AME is equivalent to a regression of the circle aver-

age on a constant term and the intervention node treatment indicator, using a spatial HAC standard error estimator and normal approximation for inference. All proofs are contained in the appendix.

We begin with the following assumptions:

C 1. (*Bernoulli design.*) (Z_1, \dots, Z_N) is a vector of *i.i.d.* $\text{Bernoulli}(p)$ draws.

C 2. (*Bounded potential outcomes.*) $|Y_x(\mathbf{z})| < b$ for some finite real constant b and all $x \in \mathcal{X}$ and $\mathbf{z} \in \mathcal{Z}$.

Assumption C1 defines the experimental design. As discussed above, condition C1 ensures that individualistic responses are *ceteris paribus* for variation in treatment assignment at a given node. We work with the assumption that the assignment probability, p , is constant over intervention nodes, although extending this to cases where assignment probabilities vary could be done by working through a suitable application of inverse probability weights (Wang, 2021). Assumption C2 is a common regularity condition on the potential outcomes that typically holds for real-world data. It ensures the boundedness of higher-order moments for the distribution of functions of the potential outcomes.

Our next assumption follows Sävje et al. (2021) by using a dependency graph to characterize interference-induced dependencies among the circle averages. Let $I_{ij}(d)$ be an indicator for whether assignment at j interferes with the d -radius circle average at i :

$$I_{ij}(d) = \begin{cases} 1 & \text{if } \mu_i(\mathbf{Y}(\mathbf{z}); d) \neq \mu_i(\mathbf{Y}(\mathbf{z}'); d) \text{ for some } \mathbf{z}, \mathbf{z}' \in \{0, 1\}^n \text{ such that } \mathbf{z}_{-j} = \mathbf{z}'_{-j} \\ 1 & \text{if } i = j, \\ 0 & \text{otherwise.} \end{cases}$$

Then, let $s_{ij}(d)$ be an indicator for whether d -radius circle averages at i and j are subject to interference from treatment at some intervention node ℓ (which could be i , j , or some other

third intervention node):

$$s_{ij}(d) = \begin{cases} 1 & \text{if } I_{\ell_i}(d)I_{\ell_j}(d) = 1 \text{ for some } \ell \in \mathcal{N}, \\ 0 & \text{otherwise .} \end{cases}$$

If $s_{ij}(d) = 1$ then circle averages at i and j will vary together whenever there is variation in treatment values at the relevant ℓ s, meaning non-independence over possible values of \mathbf{Z} .

Using this dependency graph construction, our third assumption is a restriction on the extent of interference dependencies. Let's denote the distance between two intervention nodes i and j as d_{ij} .⁵ Then we have:

C 3. (*Local interference.*) For all pairs of intervention nodes i and j in \mathcal{N} , and for distances d in the interval $[0, \bar{d}]$, there exists a constant $h(d)$ such that if $d_{ij} - d > h(d)$, then $s_{ij}(d) = 0$.

Assumption **C3** means that there are hard limits to the spatial extent of the interference: nodes that are beyond some distance from each other have no interference-induced dependencies. For intervention node j to satisfy **C3** with respect to i , it would require that the circle average of i at distance d is unaffected by not only j 's treatment value but also the treatment values at any intervention nodes that affect the circle average of j at distance d . In other words, i and j cannot share any sources of variation in their circle averages at distance d . In a spatial setting, this would typically mean that intervention nodes i and j are far apart: they neither interfere with each other nor do they have any common neighbors that interfere with them jointly. The upper bound of the interval \bar{d} defines the largest circle average radius for which this non-dependence condition might hold. Given that $h(d)$ is a hard boundary on the dependency between circle averages at i and j , **C3** implies that for i, j with $d_{ij} - d > h(d)$, $\text{Cov}[\mu_i(Y(z, \mathbf{Z}_{-i}); d), \mu_j(Y(z', \mathbf{Z}_{-j}); d)] = 0$ for all z, z' .

⁵As before, under point intervention, $d_{ij} = \|x(i) - x(j)\|$. Under polygon intervention, $d_{ij} = \min_{x \in i, x' \in j} \|x - x'\|$.

To complete our specification of the extent of interference, define the dependency neighborhood $\mathcal{B}(i; d)$ that includes all the nodes whose circle averages depend on the treatment status at node i :

$$\mathcal{B}(i; d) = \{j : d_{ij} - d \leq h(d)\}.$$

We use two terms, $c_i(d)$ and $c(d)$, to count the number of dependent circle averages for each intervention node, based on condition **C3**:

$$c_i(d) = |\{j : d_{ij} - d \leq h(d)\}| = |\mathcal{B}(i; d)|, \text{ and } c(d) = \max_{i \in \mathcal{N}} c_i(d).$$

A final assumption defines an increasing domain asymptotic growth process in which the number of independent pairs of intervention nodes increases. Our asymptotic analysis considers a sequence of sets with \mathcal{N}_N intervention nodes that reside in a corresponding sequence of sets with \mathcal{X}_N points. Define $\mathcal{N}_N(i; d) \equiv \{j \in \mathcal{N}_N : d_{ij} \leq d\}$, the set of intervention nodes whose distance to node i is not larger than d . We have the following condition on the spacing of the intervention nodes:

C 4. (*Intervention node spacing.*) For any sequence of intervention nodes, $\{i_N \in \mathcal{N}_N\}$, $\lim_{N \rightarrow \infty} \mathcal{N}_N(i_N; d) \leq b(d)$.

C4 ensures that as N grows, the number of intervention nodes that reside within a given distance of each other is uniformly bounded ([Jenish and Prucha, 2009](#), Lemma 1). It is satisfied when the intervention nodes are deliberately chosen such that they are adequately spaced out on the geography. For point-intervention experiments, we can assume that \mathcal{N}_N is a subset of an infinite countable lattice in \mathbb{R}^2 and the distance between any two points i and j on the lattice is bounded from below: $d_{ij} \geq d_0$. In practice, researchers can first divide the space into disjoint areas and select one intervention node from each area to make **C4** hold. For polygon-intervention experiments, we require that the size of each polygon is larger

than a threshold value (thus ensuring adequate spacing between non-adjacent polygons). Conditions C3 plus C4 imply that the following condition holds, which we state directly:

C 4a. (Limited local interference with respect to d .) $c(d) \leq \tilde{c}$ for any $N > 0$ and $d > 0$.

As the number of intervention nodes grows to infinity, the number of independent pairs of intervention nodes is sure to grow eventually. In our analyses below, we suppress the subscripts for asymptotic sequences unless they are needed to add clarity.

5 Estimation and inference

We begin by considering a simple contrast that serves as a Horvitz-Thompson estimator for the AME. We do so because this estimator is unbiased and provides a reference quantity in our asymptotic analysis of the more efficient Hajek estimator defined below. Consider the following Horvitz-Thompson estimator:

$$\hat{\tau}(d) = \frac{1}{Np} \sum_{i=1}^N Z_i \mu_i(\mathbf{Y}; d) - \frac{1}{N(1-p)} \sum_{i=1}^N (1 - Z_i) \mu_i(\mathbf{Y}; d). \quad (1)$$

The terms on the right-hand side consist of either known design parameters (N and p) or observable quantities. Our first two results show that $\hat{\tau}(d)$ is unbiased for $\tau(d; \eta)$ under C1 and consistent under C1-C4.

Proposition 1 (Unbiasedness). *Under C1,*

$$\tau(d; \eta) = \mathbb{E}_{\mathbf{Z}} \left[\frac{1}{Np} \sum_{i=1}^N Z_i \mu_i(\mathbf{Y}; d) - \frac{1}{N(1-p)} \sum_{i=1}^N (1 - Z_i) \mu_i(\mathbf{Y}; d) \right].$$

Proposition 2 (Asymptotic Distribution for Horvitz-Thompson). *Suppose C1-C4. Then, as $N \rightarrow \infty$,*

$$\sqrt{N}(\hat{\tau}(d) - \tau(d; \eta)) \xrightarrow{d} N(0, V_{HT}),$$

where

$$V_{HT} = \lim_{N \rightarrow \infty} N \text{Var}(\hat{\tau}(d))$$

as defined in the appendix.

The Hajek estimator is an alternative to the Horvitz-Thompson estimator, and uses, in this setting, the observed treatment and control group sizes rather than the predicted sizes (that is, $pN, (1-p)N$) that the Horvitz-Thompson estimator uses. The Hajek estimator is preferable to a Horvitz-Thompson estimator on efficiency grounds (Särndal et al., 1992, pp. 247-258). The Hajek estimator is simply the difference in the circle averages between the treated intervention nodes and control intervention nodes:

$$\hat{\tau}_{HA}(d) = \frac{1}{N_1} \sum_{i=1}^N Z_i \mu_i(\mathbf{Y}; d) - \frac{1}{N_0} \sum_{i=1}^N (1 - Z_i) \mu_i(\mathbf{Y}; d) \quad (2)$$

where $N_1 = \sum_{i=1}^N Z_i$ and $N_0 = N - N_1$.

Proposition 3 (Asymptotic Distribution for Hajek). *Suppose C1-C4. Then, as $N \rightarrow \infty$,*

$$\sqrt{N}(\hat{\tau}_{HA}(d) - \tau(d; \eta)) \xrightarrow{d} N(0, V_{HA}),$$

where

$$V_{HA} = \lim_{N \rightarrow \infty} N \text{Var}(\hat{\tau}_{HA}(d))$$

as defined in the appendix.

As a simple difference in means, the Hajek estimator can be rewritten as an ordinary least squares regression of the circle averages on a constant term and the associated intervention

nodes' treatment indicator:

$$\begin{pmatrix} \hat{\mu}_0(d) \\ \hat{\tau}_{HA}(d) \end{pmatrix} = \arg \min_{(a, \tau(d))} \sum_{i=1}^N \left[\mu_i(\mathbf{Y}; d) - \begin{pmatrix} 1 & Z_i \end{pmatrix} \begin{pmatrix} a \\ \tau(d) \end{pmatrix} \right]^2,$$

where

$$\hat{\mu}_0(d) = \frac{1}{N_0} \sum_{i=1}^N (1 - Z_i) \mu_i(\mathbf{Y}; d).$$

Our approach to variance estimation borrows from the spatial econometrics literature and works with the spatial heteroskedasticity and autocorrelation consistent (spatial HAC) variance estimator of [Conley \(1999\)](#). This estimator takes the form,

$$\hat{V} = (\mathbf{X}'\mathbf{X})^{-1} \left(\sum_{i=1}^N \sum_{j=1}^N \mathbf{X}_i \mathbf{X}_j' e_i e_j' \mathbf{1}\{j \in \mathcal{B}(i; d)\} \right) (\mathbf{X}'\mathbf{X})^{-1},$$

where

$$\mathbf{X} = \begin{pmatrix} 1, Z_1 \\ \vdots \\ 1, Z_N \end{pmatrix}, \text{ and } \mathbf{e} = \begin{pmatrix} e_1 \\ \vdots \\ e_N \end{pmatrix}$$

are the residuals from the regression. In practice, $\mathcal{B}(i; d)$ is unknown and has to be approximated by a user-chosen subset, $\{j : d_{ij} \leq \tilde{d}_i\}$. For simplicity, we can set $\tilde{d}_i = \tilde{d}$ across all the intervention nodes and examine the robustness of the results by varying the value of \tilde{d} . In the appendix, we show that the regression estimator combined with the spatial HAC variance estimator provides asymptotically conservative inference (in terms of, e.g., confidence interval coverage) for the AME under an extra assumption:

C 5. (*Homophily in treatment effects.*) For any $d \in [0, \bar{d}]$, $\frac{1}{N} \sum_{i=1}^N (\tau_i(d; \eta) - \tau(d; \eta)) \sum_{j \in \mathcal{B}(i; d)} (\tau_j(d; \eta) - \tau(d; \eta)) \geq 0$.⁶

⁶Remember that $\tau_i(d; \eta) = \mathbb{E}_{\mathbf{Z}_{-i}}[\mu_i(\mathbf{Y}(1, \mathbf{Z}_{-i}); d)] - \mathbb{E}_{\mathbf{Z}_{-i}}[\mu_i(\mathbf{Y}(0, \mathbf{Z}_{-i}); d)]$.

The assumption is that the expected treatment effect generated by node i at distance d is positively correlated with that generated by its neighbors in $\mathcal{B}(i; d)$. In other words, there is homophily in treatment effects on the space: nodes that generate larger-than-average effects reside close to each other. This kind of positive spatial correlation would seem reasonable in many applied settings—for example, when $\tau_i(d; \eta)$ varies smoothly over the intervention nodes.

Just like in scenarios without interference, the deviation of the regression-based variance from the sample-theoretic one is driven by the heterogeneity in treatment effects (Samii and Aronow, 2012; Imbens and Rubin, 2015). When interference is absent, this part is known to be negative,⁷ hence the regression-based variance estimator returns conservative variance estimates. With interference, nevertheless, this part also includes the term we defined in C5, $-\frac{1}{N} \sum_{i=1}^N (\tau_i(d; \eta) - \tau(d; \eta)) \sum_{j \in \mathcal{B}(i; d)} (\tau_j(d; \eta) - \tau(d; \eta))$, which is ensured to be negative only under this assumption. These are the reasons that the regression-based variance estimator yields conservative variance estimates.⁸ In the appendix, we demonstrate how to construct an upper bound for the sample-theoretic variance when C5 fails, as well as how to further improve the finite sample coverage of our confidence intervals with the effective degree of freedom adjustment for cluster-dependent data suggested by Young (2015).

⁷It equals $-\frac{1}{N} \sum_{i=1}^N (\tau_i - \tau)^2$, where τ_i is the individualistic treatment effect and τ is the sample average treatment effect.

⁸A similar estimator is proposed by Leung (2022b), who justifies the estimator using a super-population perspective.

6 Extensions

6.1 Structural Interpretation of the AME

Recall that the AME can be interpreted as the average effect of switching an intervention node from control to treatment, given ambient interference emanating from other intervention nodes. The degree of such ambient interference is dictated by the experimental design and in particular the level of treatment saturation (p). Generally speaking, the AME is not a structural quantity in that it may not be invariant with respect to the experimental design. Here we show that the AME can have a structural interpretation if spatial effects are additive. This particular case aligns our analysis with more standard model-based spatial analyses (Darmofal, 2015).

Suppose that for each outcome node x , its potential outcome value is generated additively:

$$Y_x(\mathbf{Z}) = \sum_{i=1}^N Z_i g_i(x) + f(x),$$

where $f(x)$ captures spatial trends in the absence of any intervention, and then $g_i(x)$ captures effects that emanate, perhaps idiosyncratically, from each of the intervention nodes. This model covers a wide variety of more restrictive models of homogenous spatial effects. It rules out that effects across intervention nodes interact, which may be an unrealistic assumption.

Under this restriction on the potential outcomes, we have that the effect of assigning treatment to an intervention node i shifts outcomes at point x by $g_i(x)$:

$$\begin{aligned} \tau_{ix}(\eta) &= E_{\mathbf{Z}_{-i}} [Y_x(1, \mathbf{Z}_{-i})] - E_{\mathbf{Z}_{-i}} [Y_x(0, \mathbf{Z}_{-i})] \\ &= E_{\mathbf{Z}_{-i}} \left[g_i(x) + \sum_{j \neq i}^N Z_j g_j(x) + f(x) \right] - E_{\mathbf{Z}_{-i}} \left[\sum_{j \neq i}^N Z_j g_j(x) + f(x) \right] \\ &= g_i(x). \end{aligned}$$

The circle-average individualistic response at distance d from intervention node i would be equal to the added effect that emanates from node i :

$$\tau_i(d; \eta) = \frac{1}{|\{x : d_i(x) = d\}|} \int_{x: d_i(x)=d} g_i(x) d\zeta.$$

Unlike the general case, this does not depend on the distribution of treatments over intervention nodes other than i . The AME for distance d is then the average of the ways that each intervention point individually affects outcomes at distance d , regardless of the treatment assignment. Thus, we could interpret the AME as a structural quantity, if we assume additive potential outcomes with no interactive effects between the intervention nodes. Whether such restrictions make sense substantively would depend on the application.

6.2 Smoothing

The estimators proposed above are nonparametric and make no assumptions about how the AME curve, $\tau(d; \eta)$, might vary in distance, d . This often yields a very jagged AME curve (as we will see below). In many applications, it is reasonable to assume that the AME curve is smooth in distance—for example when the effects are additive and smooth as in the previous section. If this is the case, for an AME at distance d , we would want to leverage information from neighboring points some small distance away.

To implement such a restriction, we can follow the approach used in [Calonico et al. \(2014\)](#) and [Hainmueller et al. \(2019\)](#) to minimize a kernel-smoothed loss function on a locally linear specification. That is, for each value of d , we solve,

$$(\widehat{a}(d), \widehat{\tau}_K(d), \widehat{\beta}(d), \widehat{\delta}(d)) = \arg \min_{(a(d), \tau(d), \beta(d), \delta(d))} \sum_{i=1}^N \sum_{d' \in \mathcal{D}} \{\mu_i(\mathbf{Y}(\mathbf{z}); d') - a(d) - \tau(d)Z_i - \beta(d)[d' - d] - \delta(d)Z_i[d' - d]\}^2 K\left(\frac{d' - d}{h}\right),$$

where $K(\cdot)$ is the chosen kernel function and h is the bandwidth. We select the optimal bandwidth via block cross-validation to minimize the estimator’s MSE (Opsomer et al., 2001) and apply the bias correction technique developed by Calonico et al. (2014) to remove the first-order asymptotic bias. Note that we have N observations for any distance value d , hence the estimator maintains the convergence rate of \sqrt{N} . As $N \rightarrow \infty$, if $h \rightarrow 0$ fast enough, the difference between the kernel regression estimator and the Hajek estimator gradually disappears, even though the former is more efficient than the latter for any fixed sample size N if smoothness holds.⁹ Consequently, the estimated $\hat{\tau}_K(d)$ is consistent for $\tau(d; \eta)$ and asymptotically normal under the same assumptions. The asymptotic variance can be estimated using a generalized spatial HAC variance estimator, with similar results as above.

6.3 Testing joint hypotheses

In our analysis above, we discussed how to construct point-wise confidence intervals for each value on the $\hat{\tau}(d; \eta)$ curve using the spatial HAC estimator and normal approximation, when sample sizes are large and the homophily condition C5 is reasonable. Researchers may also be interested in whether the effect is statistically significant on a particular interval rather than at some point. For this purpose, we propose a Fisher-style permutation test which is robust even when C5 does not hold and for smaller sample sizes.

Under the sharp null hypothesis, we know the full distribution of potential outcomes, i.e. $Y_x(\mathbf{z})$ for any \mathbf{z} . Denote the statistic of interest as $T(\mathbf{Y}, \mathbf{Z})$. Examples include estimates of each $\tau(d; \eta)$ and the average of such estimates on an interval $[d_1, d_2]$. As all the potential outcomes are known under the sharp null, we can redraw the assignment \mathbf{z} for P times and calculate the corresponding $T(\mathbf{Y}, \mathbf{Z}_p)$. The empirical distribution of $T(\mathbf{Y}, \mathbf{Z}_p)$ will approx-

⁹We leave the problems of finding the convergence rate of the optimal bandwidth and calculating the exact efficiency gain from the kernel regression estimator to future research.

imate the distribution of $T(\mathbf{Y}, \mathbf{Z})$ under the sharp null. As a result, rejecting the null if $\frac{1}{P} \sum_p \mathbf{1}\{T(\mathbf{Y}, \mathbf{Z}_p) \geq T(\mathbf{Y}, \mathbf{Z})\} \leq \alpha/2$ for some fixed large enough P gives an α -level test of significance for $T(\mathbf{Y}, \mathbf{Z})$.

An alternative is to conduct the test based on the joint distribution of $\{\hat{\tau}(d; \eta)\}_{d \in \mathcal{D}}$. Even though we can show that these estimates converge to a joint normal distribution as N grows to infinity, it is challenging to infer the variance-covariance matrix of the normal distribution due to the influence of heterogeneous treatment effects, as discussed in Section 5. Assumption C5 only allows us to bound each variance term but not the covariances. A valid, albeit highly conservative approach, would be to control type I error rates with a Bonferroni correction on the p-values. We leave this problem of testing joint hypotheses more precisely to future research.

6.4 Weaker assumptions on the extent of interference

Our proofs for Propositions 2 and 3 depend on Lemma A.1 from Ogburn et al. (2020), which actually allows for the degree of interference-based dependence to grow with N . In principle, this means that condition C3 could be weakened for similar asymptotic results to obtain. Essentially, Ogburn et al. (2020) claim that asymptotic normality follows from $\tilde{c} = o_P(N^{-1/2})$. But the convergence rate is lower than \sqrt{N} when \tilde{c} increases with the sample size and the difference between the Horvitz-Thompson and Hajek estimators gradually vanishes. Using results from Raič (2004), we can further show the joint convergence of our estimates. Another possibility is to impose restrictions on how fast the effects decline from each node, as in Kojevnikov et al. (2021) and Leung (2022a), so that there exist non-zero but small covariances between nodes that are far away from each other.

As pointed out by Sävje et al. (2021), the consistency of the Horvitz-Thompson estimator only follows from the even weaker condition of $\tilde{c} = o_P(N^{-1})$. For point interventions, we can also relate the results from Jenish and Prucha (2009) for α -mixing non-stationary random

fields on potentially unevenly spaced lattices to our setting. To do so, we define mixing conditions on the circle averages. This allows us to apply the central limit theorem from [Jenish and Prucha \(2009, Theorem 1 and Corollary 1\)](#). But applying their results would require methods for variance estimation that go beyond those we discuss in this paper. And the results do not hold for polygon interventions. We consider this an important area for further research.

7 Simulation

In this section, we use simulated datasets to illustrate propositions introduced in the previous sections and examine the performance of inferential methods based on our analytical results. We first use the hypothetical non-monotonic, additive effect function presented in [Section 3](#), which is constructed by mixing two gamma-distribution kernels. We then work with a more complex effect function that allows for interactions of effects emanating from different intervention nodes. In both scenarios, the effect’s magnitude varies across the intervention nodes. The dataset’s structure approximates our toy example in [Figure 2](#) and [Figure 3](#), but has 6400 outcome points and 64 intervention nodes. In the appendix, we describe the data generating process in details and present evidence from a simulated polygon intervention. The results are nearly identical for the polygon intervention simulation.

To get the true AME, we marginalize over all of the ways that treatment could be applied. We first calculate $\tau_{ix}(\eta)$ for each pair of (i, x) , the expectation of the effect at outcome point x induced by the treatment status’ change at intervention node i , where the expectation is taken over the treatment status at the other $N - 1$ intervention nodes. Next, we construct circle averages of $\tau_{ix}(\eta)$ using the Euclidean distance. For any distance value d , we take the average of $\tau_{ix}(\eta)$ over all the points x that fall on the edge of the circle around node i with radius d . Taking another average across all the intervention nodes renders for us $\tau(d; \eta)$ and

thus the true AME curve over values of d .

The comparison between the effect curve and the true AME curve is shown in Figure 4. On the top is the additive effect function and below is the interactive one. When effects are additive, the effect curve and the AME curve are almost identical, as expected. This follows from our analysis of the “structural interpretation” of the AME above. The interactive effect function emanating from a treated intervention node has the same shape as the additive one only when its nearest neighbor is not treated. Otherwise, it is monotonic. Therefore, the AME curve looks like the average of the non-monotonic and the monotonic effect functions.

Figure 5 illustrates the bias of the proposed estimators. We can see from the left plots that the true AME curve resides in the middle of the Hajek estimates from repeated assignments, suggesting the estimator’s bias is indeed negligible even in finite samples. Plots on the right compare the average of the 95% confidence interval endpoints constructed from the spatial HAC standard errors with the simulated 95% confidence intervals (i.e., the 2.5% and 97.5% quantiles from the permutation distribution of the effect estimates) under both the additive and the interactive effect functions. It confirms our conclusion that the spatial HAC inference is valid but slightly conservative.¹⁰

We present evidence on the proposed method’s asymptotic properties in Figure 6. Plots on the left show that the MSE of the AME estimator converges to zero at all distance values under both effect functions when the number of intervention nodes gradually rises (and the number of outcome points increases proportionally). Plots on the right show how coverage rates of the 95% confidence intervals generated by our approach vary across d and N . We can see that they are above the nominal rate of 95% when d is small and converge near it at all distance values when N is sufficiently large.

¹⁰Remember that the effect curves are smooth hence the assumption of homophily holds. As d increases, the effect gradually diminishes hence the estimated standard errors equal the simulated standard errors.

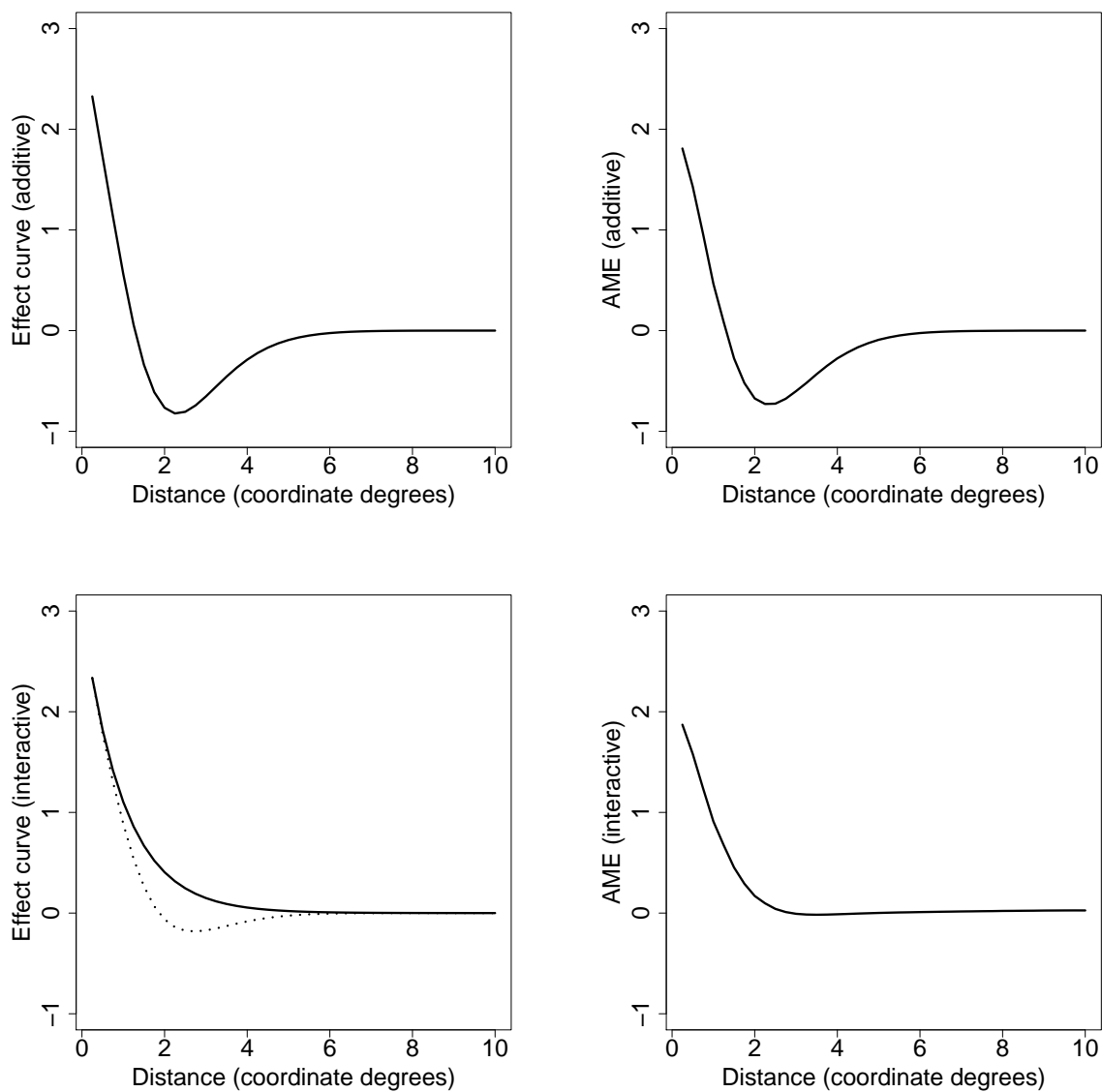


Figure 4: The comparison of the effect curve (left) and the true AME curve (right) for additive (top) and interactive (bottom) effect function.

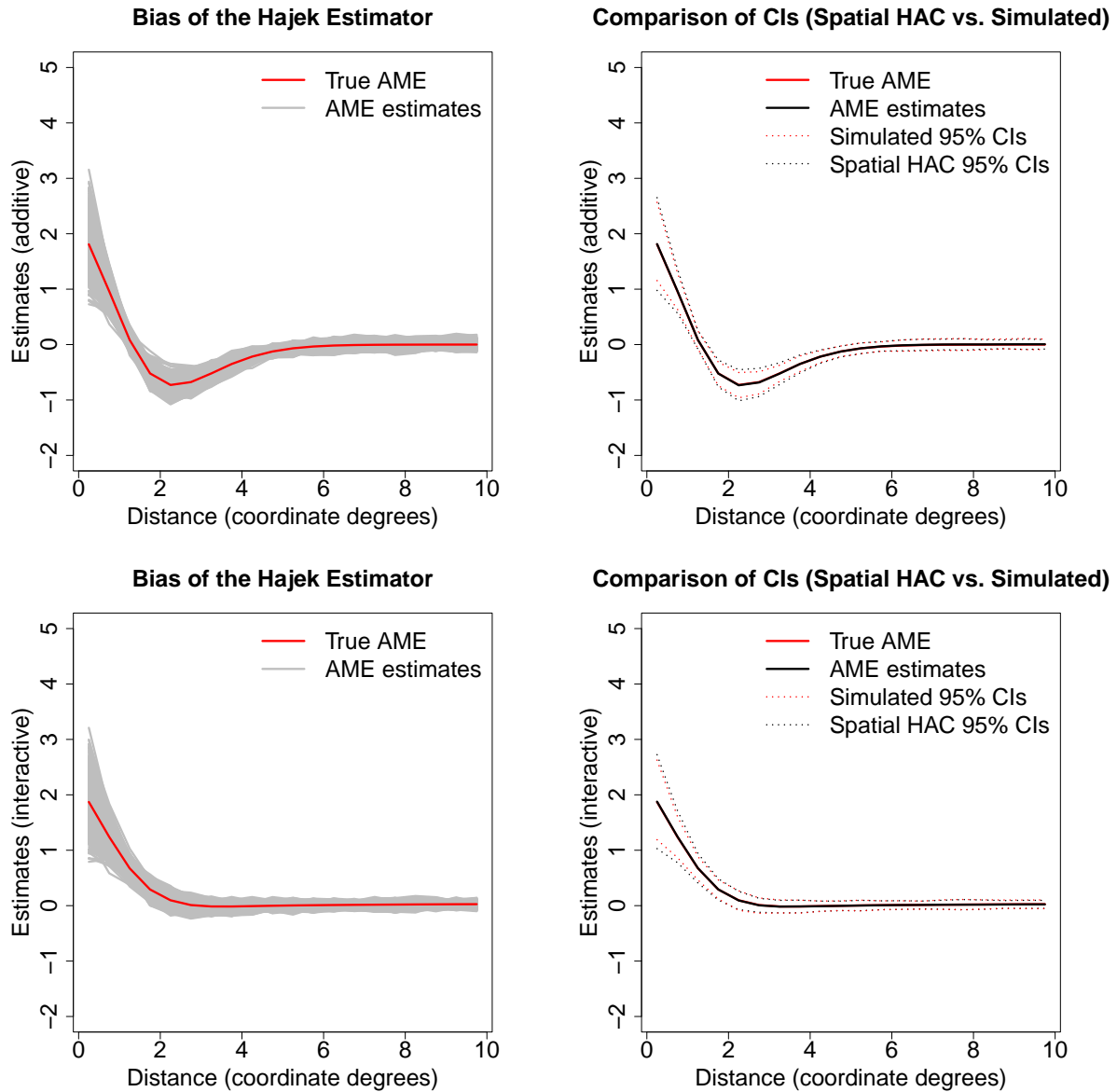


Figure 5: The bias of the Hajek estimator and the 95% spatial HAC confidence intervals under the additive (top) and interactive (bottom) effect functions. The red curves on the left figures indicate the true AME curve and each grey curve represents the Hajek estimates under one random assignment. On the right, the red dotted curves are the simulated 95% confidence intervals (i.e., the 2.5% and 97.5% quantiles of the permutation distribution) and the black dotted curves are the averages of 95% spatial HAC confidence intervals.

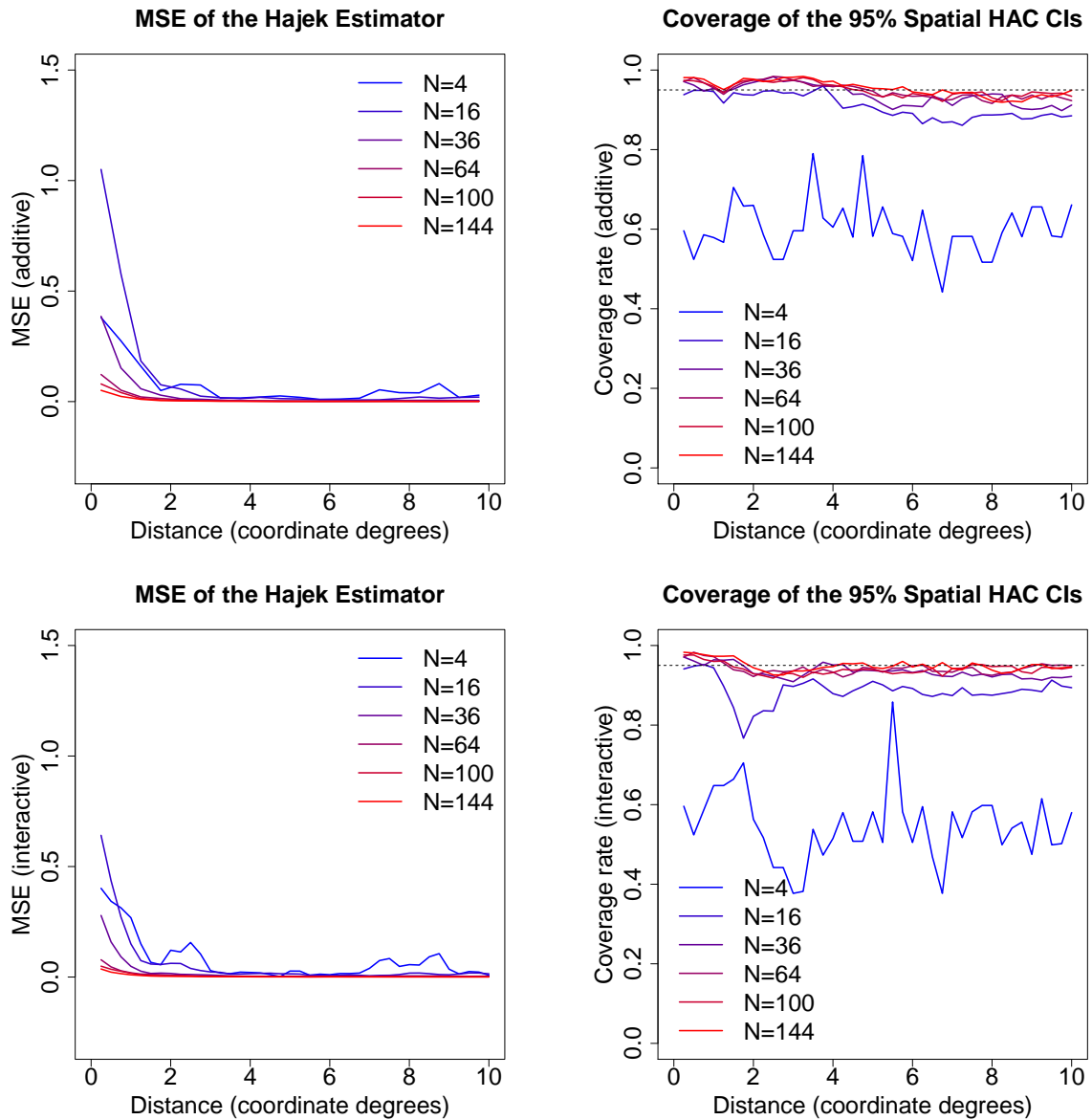


Figure 6: The top row is based on the additive effect function and the bottom one uses the interactive effect function. Each curve on the left plots shows the estimates' mean squared error (MSE) at each distance given the sample size. Plots on the right show how the average coverage rate of the 95% spatial HAC confidence interval at each distance changes with the sample size. Each curve represents the confidence interval's average coverage rate at each distance value for a given sample size. The dotted horizontal line is the nominal coverage rate (95%).

8 Examples

We demonstrate how to apply our methods in empirical studies using two examples. The first example is the study by [Miguel and Kremer \(2004\)](#) on the effects of a deworming intervention for youth in rural Kenya. In this study, pupils from 25 randomly picked schools out of 50 received deworming treatments. The left plot of [Figure 7](#) shows the spatial distribution of treated and control schools. For the present analysis, we focus on the effect of the treatment on worms infection rates.¹¹ The available data offer information on infection rates aggregated to the level of the schools. So to estimate how effects might vary over space, we used a kriging estimator to interpolate these infection rates over the entire raster surface. We then estimate the AME with these interpolated values, considering each school as an intervention node and each tile in the raster as an outcome point. Because these interpolated values vary smoothly, we calculate the circle averages using points on the edge of each circle. The range of distance values increases from 0 km to 40 km, with a step size of 1 km.

From the right plot of [Figure 7](#), we can see that the estimated effects are significantly negative when d is smaller than 2 km, whether judging from the permutation distribution under the sharp null or the spatial HAC confidence intervals. The result confirms the original finding of the paper that there exists a significant difference in infection prevalence between treated and untreated schools, even after accounting for the influence of interference. It also indicates a potentially beneficial effect diffusing outward in a small neighborhood around each intervention node. The threshold value we set for the spatial HAC variance estimator is 8 km.

The second example is the forest conservation experiment from [Jayachandran et al. \(2017\)](#). The authors evaluate the effects of a “payments for ecosystems services” (PES) program based on 121 villages in Hoima and northern Kibaale districts of Uganda. 60 vil-

¹¹The original study then went on to assess how reducing worms infections affected educational outcomes.

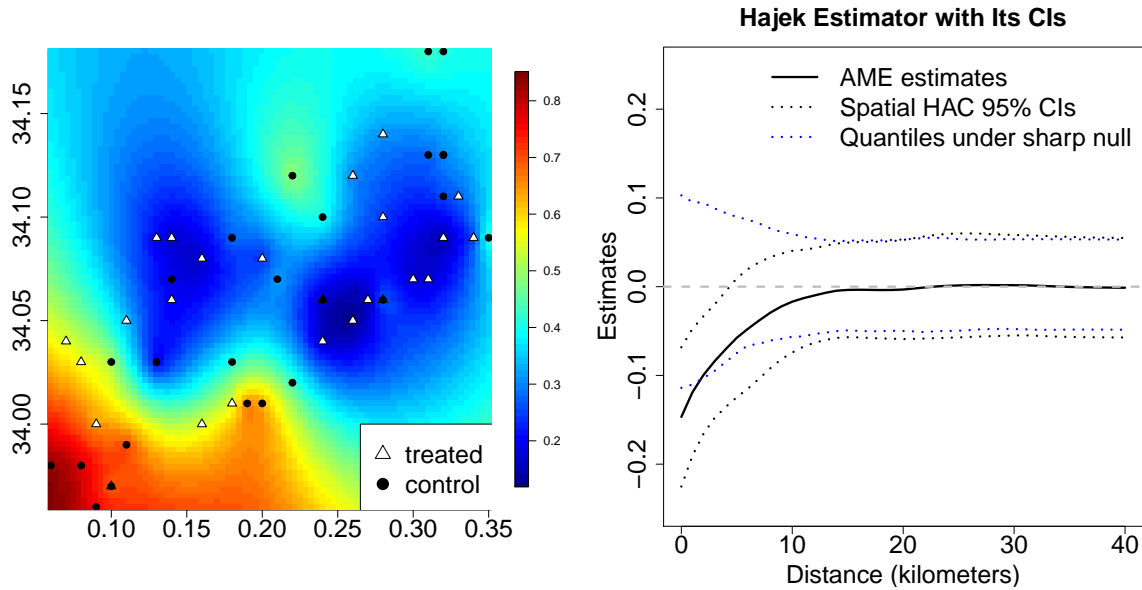


Figure 7: The plot on the left demonstrates both the treatment status of each school and interpolated outcome values from kriging in the experiment. White triangles are schools under control and black circles are treated schools. The color on the map indicates the infection rate. The plot on the right presents results using our methods. The black curve represents the AME estimate. The AME is expressed in terms of effects on the infection rate at varying distances from the schools. The black curves are 95% confidence intervals constructed from spatial HAC standard errors. The blue lines are the 2.5% and 97.5% quantiles of the effect estimates under the sharp null.

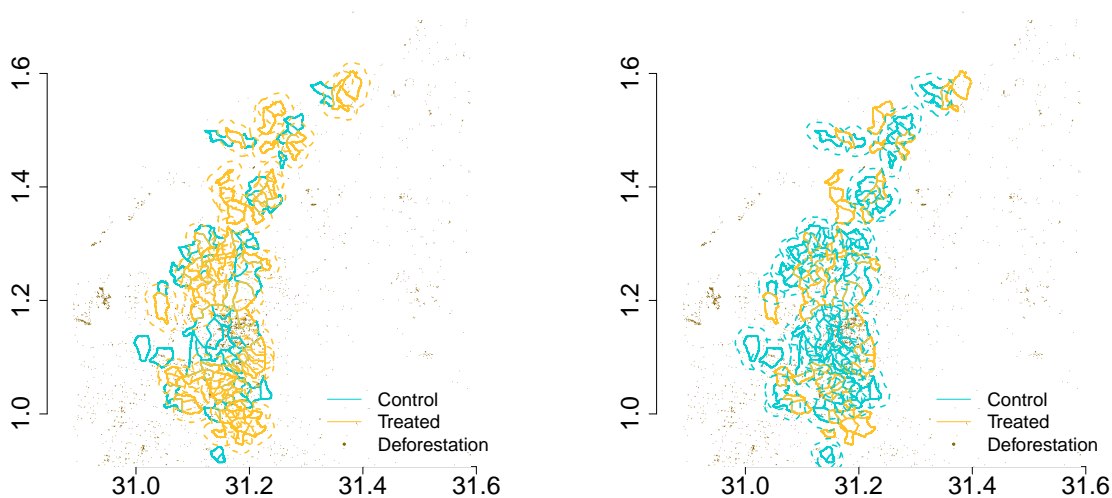


Figure 8: Both plots show the boundary of the 121 villages in [Jayachandran et al. \(2017\)](#). Villages with a golden boundary are treated and those with a turquoise boundary are under control. Dark spots on the map represent deforestation during the experiment. The left plot shows buffers around each treated village and the right one shows buffers around each untreated village.

lages were randomly assigned to the treatment group. Private forest owners in these villages were paid to reduce deforestation on their own land over a course of two years, from 2011 to 2013. Figure 8 shows the location of each village in the experiment and its treatment status. We measure the outcome of interest using the forest cover dataset from [Hansen et al. \(2013\)](#) for years 2012 and 2013, and code $Covered_{x,t}$ as 1 if raster tile x 's forest coverage rate is greater than 25% in year t , as 0 otherwise. We plot the distribution of $\Delta Covered_x = Covered_{x,2013} - Covered_{x,2012}$ in Figure 8. Dark spots on the map indicate where deforestation happened, that is, $\Delta Covered_x = 1$.

The original analysis in the paper focuses on $\Delta Covered_x$ within the boundary of the villages. We are interested in whether $\Delta Covered_x$ outside the villages is reduced by the intervention. We consider the villages as polygons rather than points due to their relative sizes on the geography. To construct the circle averages, we generate buffers around each of

the villages. For each point on a buffer, its minimal distance to the polygon in the center is the same number d , the radius of the buffer. We then take the average over all the points between two buffers (a “donut”) rather than over those on the edge of each buffer. Hence, the distance value 0 refers to the area within the boundary of the villages. To facilitate the analysis, we re-project the data onto a plane and use the Euclidean distance. The distance range is set to be between 0 km and 20 km and the threshold value is 5 km.

In Figure 9, plots on the left report results from the Hajek estimator, and plots on the right report results from the kernel regression estimator. On the top, we show the AME estimates and their 95% confidence intervals as curves. On the bottom, we present them as coefficient estimates. Both estimators detect a significant decrease of deforestation within the boundary of the villages, even though the magnitude is smaller than what the authors reported.¹² We also find evidence of spillover effects in space. It is harder to tell from the Hajek estimates as their values are more jagged across distance values. But from the estimates generated by the kernel regression estimator, we can see that the effect is significant at the 10% level for areas which within 2 km of the boundary of the treated villages. Our permutation test confirms the conclusion. We show in the appendix that the results are robust to a range of threshold values.

9 Conclusion

When treatments are applied at given intervention nodes in space, the effects may bleed out in complex ways. Moreover, effects that bleed out from multiple nodes may interact with each other. As a result, the spatial effects at any point can depend on the entire distribution of treatments over intervention nodes, rather than on the treatment status

¹²A possible reason is that the data the authors used came from a commercial satellite company, which has a higher resolution than ours.

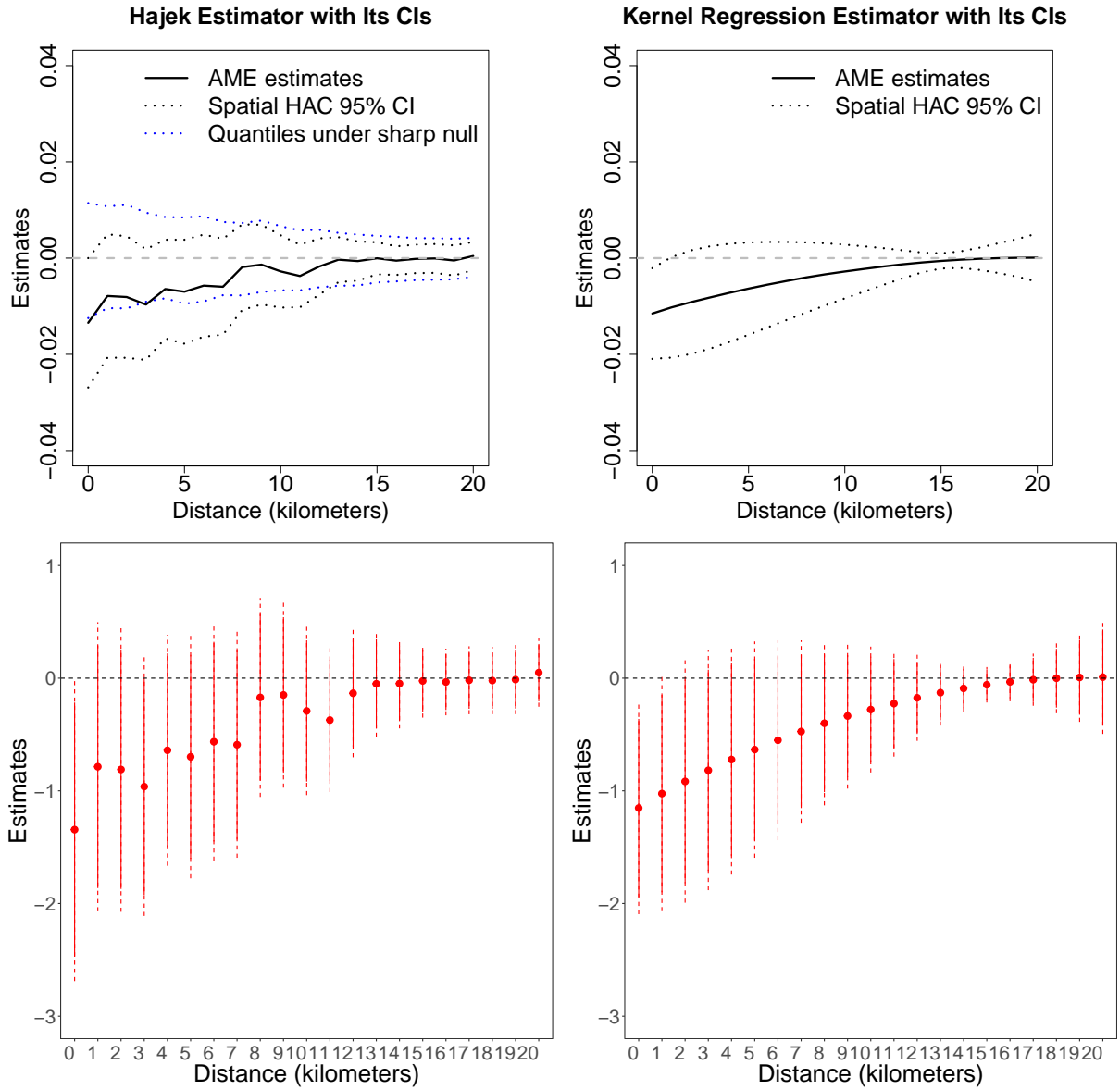


Figure 9: Plots on the left present results from the Hajek estimator, while plots on the right present those from the kernel regression estimator. On the top, the effects and their 95% confidence intervals are shown as curves. The black solid line represents the estimated AME at each distance value. The black dotted lines around it are the 95% spatial HAC confidence intervals. The blue dotted lines are the 2.5% and 97.5% quantiles of the effect estimates under the sharp null. On the bottom are coefficients plots. The solid segments mark the 95% spatial HAC confidence intervals and the dotted ones mark the 90% spatial HAC confidence intervals.

of only the nearest node. To capture such effects adequately, one needs to account for such interference appropriately. Standard approaches, which ignore such interference, yield conclusions about average policy impacts that may be unwarranted.

This paper explains how one can account for such interference in a randomized spatial experiment and estimate a meaningful spatial effect—what we call the “average marginalized effect” (AME). The AME tells us what would happen, on average, if we switch an intervention node at a given distance into treatment, averaging over ambient effects emanating from other intervention nodes. We can construct AME estimates for difference distances, yielding a spatial effect curve. The AME is identified under random assignment as a simple contrast. Under restrictions on the spatial extent of interference, we can estimate the AME consistently and perform accurate inference using simple difference-in-means estimators and readily-available spatial standard error estimators.

We also develop a number of extensions. This includes the specification of conditions under which the AME can be interpreted as a structural quantity that does not depend on the experimental design. We offer an approach for potentially increasing statistical power by allowing for smoothing over distance, and explain how to test hypotheses on joint effects using Fisher-style permutation under the sharp null.

We illustrate our approach using simulation and two examples from real-world spatial experiments. The examples show the soundness of our proposed methods but also point to areas for refinement in further research. These include introducing methods to boost power, for example, by incorporating spatial covariate information, and to further improve finite sample inference.

A Analytical results

We first prove the unbiasedness of the Horvitz-Thompson estimator for the AME. We then characterize the variance of the Horvitz-Thompson estimator and the Hajek estimator, as well as their rates of convergence. We put all of these pieces together to prove the results for asymptotic distributions. Finally, we show that the regression-based approach using the spatial HAC standard errors provides for conservative inference.

A.1 Lemmas

We first state a lemma for the analysis that follows.

Lemma A.1. *For any function $f : \{0, 1\}^N \rightarrow \mathbb{R}$, assuming C1, we have:*

C1.1 $E [Z_i^k f(\mathbf{Z})] = p E_{\mathbf{Z}_{-i}} [f(1, \mathbf{Z}_{-i})]$ for any integer k ¹³.

C1.2 $E [Z_i^k Z_j^l f(\mathbf{Z})] = p^2 E_{\mathbf{Z}_{-(i,j)}} [f(1, 1, \mathbf{Z}_{-(i,j)})]$ for any integer k and l .

Proof. By Law of Iterated Expectations. □

¹³Without further notification, the expectation is always taken over \mathbf{Z} in what follows.

A.2 Proposition 1 (Horvitz-Thompson Unbiasedness)

Proof. Recall the definition of the Horvitz-Thompson estimator in (1): $\hat{\tau}(d) = \frac{1}{Np} \sum_{i=1}^N Z_i \mu_i(\mathbf{Y}; d) - \frac{1}{N(1-p)} \sum_{i=1}^N (1 - Z_i) \mu_i(\mathbf{Y}; d)$.

$$\begin{aligned}
\tau(d; \eta) &= \frac{1}{N} \sum_{i=1}^N \mu_i(1; d, \eta) - \frac{1}{N} \sum_{i=1}^N \mu_i(0; d, \eta) \\
&= \frac{1}{Np} \sum_{i=1}^N p \mathbb{E}_{\mathbf{z}_{-i}} [\mu_i(\mathbf{Y}(1, \mathbf{Z}_{-i}); d)] - \frac{1}{N(1-p)} \sum_{i=1}^N (1-p) \mathbb{E}_{\mathbf{z}_{-i}} [\mu_i(\mathbf{Y}(0, \mathbf{Z}_{-i}); d)] \\
&= \frac{1}{Np} \sum_{i=1}^N \mathbb{E}_{\mathbf{z}} [Z_i \mu_i(\mathbf{Y}; d)] - \frac{1}{N(1-p)} \sum_{i=1}^N \mathbb{E}_{\mathbf{z}} [(1 - Z_i) \mu_i(\mathbf{Y}; d)] \\
&= \mathbb{E}_{\mathbf{z}} \left[\frac{1}{Np} \sum_{i=1}^N Z_i \mu_i(\mathbf{Y}; d) - \frac{1}{N(1-p)} \sum_{i=1}^N (1 - Z_i) \mu_i(\mathbf{Y}; d) \right],
\end{aligned}$$

where the second equality uses the definition of $\mu_i(z; d, \eta)$, the third equality follows from Lemma A.1. □

We now characterize the variance of the Horvitz-Thompson estimator.

Lemma A.2. *Under conditions C1-C3 as defined in the main text, the variance of estimator $\hat{\tau}(d)$ is bounded as follows:*

$$\begin{aligned}
&\text{Var}(\hat{\tau}(d)) \\
&\leq \frac{1}{N^2 p} \sum_{i=1}^N \mathbb{E} [\mu_i^2(\mathbf{Y}(1, \mathbf{Z}_{-i}); d)] + \frac{1}{N^2 (1-p)} \sum_{i=1}^N \mathbb{E} [\mu_i^2(\mathbf{Y}(0, \mathbf{Z}_{-i}); d)] \\
&\quad + \frac{1}{N^2} \sum_{i=1}^N \sum_{j \in \mathcal{B}(i; d)} \sum_{a, b=0}^1 (-1)^{a+b} \left\{ \mathbb{E} [\mu_i(\mathbf{Y}(a, b, \mathbf{Z}_{-(i,j)}); d) \mu_j(\mathbf{Y}(a, b, \mathbf{Z}_{-(i,j)}); d)] \right. \\
&\quad \left. - \mathbb{E} [\mu_i(\mathbf{Y}(a, \mathbf{Z}_{-i}); d)] \mathbb{E} [\mu_j(\mathbf{Y}(b, \mathbf{Z}_{-j}); d)] \right\},
\end{aligned}$$

and we have that

$$\text{Var}(\hat{\tau}(d)) = O\left(\frac{1}{N}\right).$$

Proof. Using the expression of the Horvitz-Thompson estimator, we have:

$$\begin{aligned} & \text{Var}(\hat{\tau}(d)) \\ &= \frac{1}{N^2} \text{Var} \left[\sum_{i=1}^N \left(\frac{Z_i}{p} - \frac{1-Z_i}{1-p} \right) \mu_i(\mathbf{Y}(\mathbf{Z}); d) \right] \\ &= \frac{1}{N^2} \sum_{i=1}^N \text{Var} \left[\left(\frac{Z_i}{p} - \frac{1-Z_i}{1-p} \right) \mu_i(\mathbf{Y}(\mathbf{Z}); d) \right] \\ & \quad + \frac{1}{N^2} \sum_{i=1}^N \sum_{j \neq i} \text{Cov} \left[\left(\frac{Z_i}{p} - \frac{1-Z_i}{1-p} \right) \mu_i(\mathbf{Y}(\mathbf{Z}); d), \left(\frac{Z_j}{p} - \frac{1-Z_j}{1-p} \right) \mu_j(\mathbf{Y}(\mathbf{Z}); d) \right] \\ &= \frac{1}{N^2} \sum_{i=1}^N \text{E} \left[\left(\left(\frac{Z_i}{p} - \frac{1-Z_i}{1-p} \right) \mu_i(\mathbf{Y}(\mathbf{Z}); d) \right)^2 \right] - \frac{1}{N^2} \sum_{i=1}^N \left(\text{E} \left[\left(\frac{Z_i}{p} - \frac{1-Z_i}{1-p} \right) \mu_i(\mathbf{Y}(\mathbf{Z}); d) \right] \right)^2 \\ & \quad + \frac{1}{N^2} \sum_{i=1}^N \sum_{j \neq i} \text{Cov} \left[\frac{Z_i}{p} \mu_i(\mathbf{Y}(\mathbf{Z}); d), \frac{Z_j}{p} \mu_j(\mathbf{Y}(\mathbf{Z}); d) \right] \\ & \quad - \frac{1}{N^2} \sum_{i=1}^N \sum_{j \neq i} \text{Cov} \left[\frac{Z_i}{p} \mu_i(\mathbf{Y}(\mathbf{Z}); d), \frac{1-Z_j}{1-p} \mu_j(\mathbf{Y}(\mathbf{Z}); d) \right] \\ & \quad - \frac{1}{N^2} \sum_{i=1}^N \sum_{j \neq i} \text{Cov} \left[\frac{1-Z_i}{1-p} \mu_i(\mathbf{Y}(\mathbf{Z}); d), \frac{Z_j}{p} \mu_j(\mathbf{Y}(\mathbf{Z}); d) \right] \\ & \quad + \frac{1}{N^2} \sum_{i=1}^N \sum_{j \neq i} \text{Cov} \left[\frac{1-Z_i}{1-p} \mu_i(\mathbf{Y}(\mathbf{Z}); d), \frac{1-Z_j}{1-p} \mu_j(\mathbf{Y}(\mathbf{Z}); d) \right]. \end{aligned}$$

We further expand the first two terms in the above expression:

$$\begin{aligned}
& \frac{1}{N^2} \sum_{i=1}^N \mathbb{E} \left[\left(\left(\frac{Z_i}{p} - \frac{1-Z_i}{1-p} \right) \mu_i(\mathbf{Y}(\mathbf{Z}); d) \right)^2 \right] - \frac{1}{N^2} \sum_{i=1}^N \mathbb{E} \left[\left(\frac{Z_i}{p} - \frac{1-Z_i}{1-p} \right) \mu_i(\mathbf{Y}(\mathbf{Z}); d) \right]^2 \\
&= \frac{1}{N^2} \sum_{i=1}^N \mathbb{E} \left[\frac{Z_i^2}{p^2} \mu_i^2(\mathbf{Y}(\mathbf{Z}); d) \right] + \frac{1}{N^2} \sum_{i=1}^N \mathbb{E} \left[\frac{(1-Z_i)^2}{(1-p)^2} \mu_i^2(\mathbf{Y}(\mathbf{Z}); d) \right] \\
&\quad - \frac{1}{N^2} \sum_{i=1}^N \mathbb{E}^2 \left[\left(\frac{Z_i}{p} - \frac{1-Z_i}{1-p} \right) \mu_i(\mathbf{Y}(\mathbf{Z}); d) \right] \\
&= \frac{1}{N^2 p} \sum_{i=1}^N \mathbb{E} [\mu_i^2(\mathbf{Y}(1, \mathbf{Z}_{-i}); d)] + \frac{1}{N^2(1-p)} \sum_{i=1}^N \mathbb{E} [\mu_i^2(\mathbf{Y}(0, \mathbf{Z}_{-i}); d)] \\
&\quad - \frac{1}{N^2} \sum_{i=1}^N \mathbb{E}^2 [\mu_i(\mathbf{Y}(1, \mathbf{Z}_{-i}); d) - \mu_i(\mathbf{Y}(0, \mathbf{Z}_{-i}); d)] \\
&\leq \frac{1}{N^2 p} \sum_{i=1}^N \mathbb{E} [\mu_i^2(\mathbf{Y}(1, \mathbf{Z}_{-i}); d)] + \frac{1}{N^2(1-p)} \sum_{i=1}^N \mathbb{E} [\mu_i^2(\mathbf{Y}(0, \mathbf{Z}_{-i}); d)].
\end{aligned}$$

We also have:

$$\begin{aligned}
& \frac{1}{Np} \sum_{i=1}^N \mathbb{E} [\mu_i^2(\mathbf{Y}(1, \mathbf{Z}_{-i}); d)] + \frac{1}{N(1-p)} \sum_{i=1}^N \mathbb{E} [\mu_i^2(\mathbf{Y}(0, \mathbf{Z}_{-i}); d)] \\
&\quad - \frac{1}{N} \sum_{i=1}^N \mathbb{E}^2 [\mu_i(\mathbf{Y}(1, \mathbf{Z}_{-i}); d) - \mu_i(\mathbf{Y}(0, \mathbf{Z}_{-i}); d)] = O(1),
\end{aligned}$$

since C2 implies that all the moments are bounded. Next, we examine the first covariance

term, which equals

$$\begin{aligned}
& \frac{1}{N^2} \sum_{i=1}^N \sum_{j \neq i} \text{Cov} \left[\frac{Z_i}{p} \mu_i(\mathbf{Y}(\mathbf{Z}); d), \frac{Z_j}{p} \mu_j(\mathbf{Y}(\mathbf{Z}); d) \right] \\
&= \frac{1}{N^2} \sum_{i=1}^N \sum_{j \neq i} \text{E} \left[\frac{Z_i Z_j}{p^2} \mu_i(\mathbf{Y}(\mathbf{Z}); d) \mu_j(\mathbf{Y}(\mathbf{Z}); d) \right] \\
&\quad - \frac{1}{N^2} \sum_{i=1}^N \sum_{j \neq i} \text{E} \left[\frac{Z_i}{p} \mu_i(\mathbf{Y}(\mathbf{Z}); d) \right] \text{E} \left[\frac{Z_j}{p} \mu_j(\mathbf{Y}(\mathbf{Z}); d) \right] \\
&= \frac{1}{N^2} \sum_{i=1}^N \sum_{j \neq i} \text{E} \left[\mu_i(\mathbf{Y}(1, 1, \mathbf{Z}_{-(i,j)}); d) \mu_j(\mathbf{Y}(1, 1, \mathbf{Z}_{-(i,j)}); d) \right] \\
&\quad - \frac{1}{N^2} \sum_{i=1}^N \sum_{j \neq i} \text{E} \left[\mu_i(\mathbf{Y}(1, \mathbf{Z}_{-i}); d) \right] \text{E} \left[\mu_j(\mathbf{Y}(1, \mathbf{Z}_{-i}); d) \right] \\
&= \frac{1}{N^2} \sum_{i=1}^N \sum_{j \in \mathcal{B}(i;d)} \text{E} \left[\mu_i(\mathbf{Y}(1, 1, \mathbf{Z}_{-(i,j)}); d) \mu_j(\mathbf{Y}(1, 1, \mathbf{Z}_{-(i,j)}); d) \right] \\
&\quad - \frac{1}{N^2} \sum_{i=1}^N \sum_{j \in \mathcal{B}(i;d)} \text{E} \left[\mu_i(\mathbf{Y}(1, \mathbf{Z}_{-i}); d) \right] \text{E} \left[\mu_j(\mathbf{Y}(1, \mathbf{Z}_{-i}); d) \right].
\end{aligned}$$

The last equality holds because of assumption C3 on local interference. For $j \notin \mathcal{B}(i)$, $\mu_i(\mathbf{Y}(1, 1, \mathbf{Z}_{-(i,j)}); d) = \mu_i(\mathbf{Y}(1, \mathbf{Z}_{-i}); d)$ and $\text{E} \left[\mu_i(\mathbf{Y}(1, 1, \mathbf{Z}_{-(i,j)}); d) \mu_j(\mathbf{Y}(1, 1, \mathbf{Z}_{-(i,j)}); d) \right] = \text{E} \left[\mu_i(\mathbf{Y}(1, 1, \mathbf{Z}_{-(i,j)}); d) \right] \text{E} \left[\mu_j(\mathbf{Y}(1, 1, \mathbf{Z}_{-(i,j)}); d) \right]$, following the definition of interference in Section 4. Moreover,

$$\begin{aligned}
& \frac{1}{N} \sum_{i=1}^N \sum_{j \in \mathcal{B}(i;d)} \text{E} \left[\mu_i(\mathbf{Y}(1, 1, \mathbf{Z}_{-(i,j)}); d) \mu_j(\mathbf{Y}(1, 1, \mathbf{Z}_{-(i,j)}); d) \right] \\
&\quad - \frac{1}{N} \sum_{i=1}^N \sum_{j \in \mathcal{B}(i;d)} \text{E} \left[\mu_i(\mathbf{Y}(1, \mathbf{Z}_{-i}); d) \right] \text{E} \left[\mu_j(\mathbf{Y}(1, \mathbf{Z}_{-i}); d) \right] = O(1),
\end{aligned}$$

since $|\mathcal{B}(i;d)|$ is bounded from above by \tilde{c} . Other covariance terms have similar forms. We obtain the bound of the variance and its convergence rate by combining these terms together. \square

Next, we derive the limiting variance of the Hajek estimator using linearization.

Lemma A.3. *Consider the estimator $\widehat{\tau}_{HA}(d)$ defined in (2). It has the following asymptotic linear expansion:*

$$\begin{aligned} \widehat{\tau}_{HA}^{Taylor}(d) &= \bar{\mu}^1(d) - \bar{\mu}^0(d) + \frac{1}{Np} \sum_{i=1}^N Z_i (\mu_i(\mathbf{Y}(\mathbf{Z}); d) - \bar{\mu}^1(d)) \\ &\quad - \frac{1}{Np} \sum_{i=1}^N (1 - Z_i) (\mu_i(\mathbf{Y}(\mathbf{Z}); d) - \bar{\mu}^0(d)), \end{aligned}$$

where $\bar{\mu}^1(d) = \frac{1}{N} \sum_{i=1}^N \mathbb{E} [\mu_i(\mathbf{Y}(1, \mathbf{Z}_{-i}); d)]$ and $\bar{\mu}^0(d) = \frac{1}{N} \sum_{i=1}^N \mathbb{E} [\mu_i(\mathbf{Y}(0, \mathbf{Z}_{-i}); d)]$. Such an expansion satisfies

$$\sqrt{N}(\widehat{\tau}_{HA}^{Taylor}(d) - \widehat{\tau}_{HA}(d)) = o_p(1).$$

Proof. Denote $\hat{\mu}^1(d) = \frac{1}{Np} \sum_{i=1}^N Z_i \mu_i(\mathbf{Y}(\mathbf{Z}); d)$, $\hat{\mu}^0(d) = \frac{1}{N(1-p)} \sum_{i=1}^N (1 - Z_i) \mu_i(\mathbf{Y}(\mathbf{Z}); d)$, $\hat{N}_1 = \frac{\sum_{i=1}^N Z_i}{Np}$, $\hat{N}_0 = \frac{\sum_{i=1}^N (1 - Z_i)}{N(1-p)}$, and $\mathbf{W} = (\hat{\mu}^1(d), \hat{\mu}^0(d), \hat{N}_1, \hat{N}_0)$.

We know that $\mathbb{E} [\hat{\mu}^1(d)] = \bar{\mu}^1(d)$, $\mathbb{E} [\hat{\mu}^0(d)] = \bar{\mu}^0(d)$, $\mathbb{E} [\hat{N}_1] = \mathbb{E} [\hat{N}_0] = 1$. Thus, $\mathbb{E} [\mathbf{W}] = (\bar{\mu}^1(d), \bar{\mu}^0(d), 1, 1)$. Define $f(a, b, c, d) = \frac{a}{c} - \frac{b}{d}$. Then the Hajek estimator can be written as $f(\mathbf{W}) = f(\hat{\mu}^1(d), \hat{\mu}^0(d), \hat{N}_1, \hat{N}_0)$.

With probability approaching 1, we have the following Taylor expansion of the Hajek estimator:

$$\begin{aligned} \sqrt{N} \widehat{\tau}_{HA}(d) &= \sqrt{N} f(\hat{\mu}^1(d), \hat{\mu}^0(d), \hat{N}_1, \hat{N}_0) = \sqrt{N} f(\mathbf{W}) \\ &= \sqrt{N} f(\mathbb{E} [\mathbf{W}]) + \sqrt{N} \left. \frac{\partial f}{\partial \mathbf{W}} \right|_{\mathbf{W}=\mathbb{E}[\mathbf{W}]} (\mathbf{W} - \mathbb{E} [\mathbf{W}]) + o_P(\sqrt{N} \|\mathbf{W} - \mathbb{E} [\mathbf{W}]\|). \end{aligned}$$

We know that $\sqrt{N} \|\mathbf{W} - \mathbb{E} [\mathbf{W}]\| = O_p(1)$ following the same argument as in Lemma A.2. Hence, $o_P(\sqrt{N} \|\mathbf{W} - \mathbb{E} [\mathbf{W}]\|) = o_p(1)$. It is easy to see that $\left. \frac{\partial f}{\partial \mathbf{W}} \right|_{\mathbb{E}[\mathbf{W}]} = (1, -1, -\bar{\mu}^1(d), \bar{\mu}^0(d))'$. Some algebraic manipulations prove that the first two terms sim-

ply to the expressions in $\hat{\tau}_{HA}^{Taylor}(d)$. □

Lemma A.4. *The variance of the linearized Hajek estimator can be expressed as*

$$\begin{aligned}
& \text{Var} \left(\hat{\tau}_{HA}^{Taylor}(d) \right) \\
&= \frac{1}{N^2 p} \sum_{i=1}^N \text{E} \left[(\mu_i(\mathbf{Y}(1, \mathbf{Z}_{-i}); d) - \bar{\mu}^1)^2 \right] + \frac{1}{N^2(1-p)} \sum_{i=1}^N \text{E} \left[(\mu_i(\mathbf{Y}(0, \mathbf{Z}_{-i}); d) - \bar{\mu}^0)^2 \right] \\
&- \frac{1}{N^2} \sum_{i=1}^N \text{E}^2 \left[\mu_i(\mathbf{Y}(1, \mathbf{Z}_{-i}); d) - \bar{\mu}^1(d) \right] - \frac{1}{N^2} \sum_{i=1}^N \text{E}^2 \left[\mu_i(\mathbf{Y}(0, \mathbf{Z}_{-i}); d) - \bar{\mu}^0(d) \right] \\
&+ \frac{1}{N^2} \sum_{i=1} \sum_{j \in \mathcal{B}(i;d)} \sum_{a,b=0}^1 (-1)^{a+b} \text{E} \left[(\mu_i(\mathbf{Y}(a, b, \mathbf{Z}_{-(i,j)}); d) - \bar{\mu}^a(d)) (\mu_j(\mathbf{Y}(a, b, \mathbf{Z}_{-(i,j)}); d) - \bar{\mu}^b(d)) \right] \\
&- \frac{1}{N^2} \sum_{i=1} \sum_{j \in \mathcal{B}(i;d)} \sum_{a,b=0}^1 (-1)^{a+b} \text{E} \left[\mu_i(\mathbf{Y}(a, \mathbf{Z}_{-i}); d) - \bar{\mu}^a(d) \right] \text{E} \left[\mu_j(\mathbf{Y}(b, \mathbf{Z}_{-j}); d) - \bar{\mu}^b(d) \right],
\end{aligned} \tag{3}$$

Under conditions C1-C5, we have the following variance bound for $\text{Var} \left(\hat{\tau}_{HA}^{Taylor}(d) \right)$:

$$\begin{aligned}
\tilde{V} &= \frac{1}{N^2 p} \sum_{i=1}^N \text{E} \left[(\mu_i(\mathbf{Y}(1, \mathbf{Z}_{-i}); d) - \bar{\mu}^1)^2 \right] + \frac{1}{N^2(1-p)} \sum_{i=1}^N \text{E} \left[(\mu_i(\mathbf{Y}(0, \mathbf{Z}_{-i}); d) - \bar{\mu}^0)^2 \right] \\
&+ \frac{1}{N^2} \sum_{i=1} \sum_{j \in \mathcal{B}(i;d)} \sum_{a,b=0}^1 (-1)^{a+b} \text{E} \left[(\mu_i(\mathbf{Y}(a, b, \mathbf{Z}_{-(i,j)}); d) - \bar{\mu}^a(d)) (\mu_j(\mathbf{Y}(a, b, \mathbf{Z}_{-(i,j)}); d) - \bar{\mu}^b(d)) \right].
\end{aligned}$$

Proof. Recalling the definitions of \mathbf{W} and $f(\cdot)$ from the proof of Lemma A.3, we first characterize the variance of the linearized Hajek estimator is:

$$\begin{aligned}
\text{Var} \left(\hat{\tau}_{HA}^{Taylor}(d) \right) &= \text{E} \left[\left. \frac{\partial f}{\partial \mathbf{W}} \right|_{\mathbf{w}=\text{E}[\mathbf{W}]}' * (\mathbf{W} - \text{E}[\mathbf{W}]) \right]^2 \\
&= \left(\left. \frac{\partial f}{\partial \mathbf{W}} \right|_{\text{E}[\mathbf{W}]} \right)' \text{Var}[\mathbf{W}] \left. \frac{\partial f}{\partial \mathbf{W}} \right|_{\text{E}[\mathbf{W}]}
\end{aligned}$$

Further,

$$\text{Var} [\mathbf{W}] = \begin{pmatrix} \text{Var} [\hat{\mu}^1(d)] & \text{Cov} [\hat{\mu}^1(d), \hat{\mu}^0(d)] & \text{Cov} [\hat{\mu}^1(d), \hat{N}_1] & \text{Cov} [\hat{\mu}^1(d), \hat{N}_0] \\ \text{Cov} [\hat{\mu}^1(d), \hat{\mu}^0(d)] & \text{Var} [\hat{\mu}^0(d)] & \text{Cov} [\hat{\mu}^0(d), \hat{N}_1] & \text{Cov} [\hat{\mu}^0(d), \hat{N}_0] \\ \text{Cov} [\hat{\mu}^1(d), \hat{N}_1] & \text{Cov} [\hat{\mu}^0(d), \hat{N}_1] & \text{Var} [\hat{N}_1] & \text{Cov} [\hat{N}_1, \hat{N}_0] \\ \text{Cov} [\hat{\mu}^1(d), \hat{N}_0] & \text{Cov} [\hat{\mu}^0(d), \hat{N}_0] & \text{Cov} [\hat{N}_1, \hat{N}_0] & \text{Var} [\hat{N}_0] \end{pmatrix}$$

Therefore,

$$\begin{aligned} & \left(\frac{\partial f}{\partial \mathbf{W}} \Big|_{\mathbb{E}[\mathbf{W}]} \right)' \text{Var} [\mathbf{W}] \frac{\partial f}{\partial \mathbf{W}} \Big|_{\mathbb{E}[\mathbf{W}]} \\ &= \text{Var} [\hat{\mu}^1(d)] + \text{Var} [\hat{\mu}^0(d)] + (\bar{\mu}^1(d))^2 \text{Var} [\hat{N}_1] + (\bar{\mu}^0(d))^2 \text{Var} [\hat{N}_0] \\ & \quad - 2\text{Cov} [\hat{\mu}^1(d), \hat{\mu}^0(d)] - 2\bar{\mu}^1(d)\text{Cov} [\hat{\mu}^1(d), \hat{N}_1] + 2\bar{\mu}^0(d)\text{Cov} [\hat{\mu}^1(d), \hat{N}_0] \\ & \quad + 2\bar{\mu}^1(d)\text{Cov} [\hat{\mu}^0(d), \hat{N}_1] - 2\bar{\mu}^0(d)\text{Cov} [\hat{\mu}^0(d), \hat{N}_0] - 2(\bar{\mu}^1(d)\bar{\mu}^0(d)) \text{Cov} [\hat{N}_1, \hat{N}_0] \\ &= \text{Var} [\hat{\mu}^1(d) - \bar{\mu}^1(d)\hat{N}_1] + \text{Var} [\hat{\mu}^0(d) - \bar{\mu}^0(d)\hat{N}_0] \\ & \quad - 2\text{Cov} [\hat{\mu}^1(d) - \bar{\mu}^1(d)\hat{N}_1, \hat{\mu}^0(d) - \bar{\mu}^0(d)\hat{N}_0]. \end{aligned}$$

For the term $\text{Var} \left[\hat{\mu}^1(d) - \bar{\mu}^1(d) \hat{N}_1 \right]$, we have:

$$\begin{aligned}
& \text{Var} \left[\hat{\mu}^1(d) - \bar{\mu}^1(d) \hat{N}_1 \right] = \frac{1}{N^2 p^2} \text{Var} \left[\sum_{i=1}^N Z_i (\mu_i(\mathbf{Y}(\mathbf{Z}); d) - \bar{\mu}^1(d)) \right] \\
&= \frac{1}{N^2 p^2} \sum_{i=1}^N \text{Var} [Z_i (\mu_i(\mathbf{Y}(\mathbf{Z}); d) - \bar{\mu}^1(d))] \\
&\quad + \frac{1}{N^2 p^2} \sum_{i=1}^N \sum_{j \neq i}^N \text{Cov} [Z_i (\mu_i(\mathbf{Y}(\mathbf{Z}); d) - \bar{\mu}^1(d)), Z_j (\mu_j(\mathbf{Y}(\mathbf{Z}); d) - \bar{\mu}^1(d))] \\
&= \frac{1}{N^2 p^2} \sum_{i=1}^N \text{E} [Z_i (\mu_i(\mathbf{Y}(\mathbf{Z}); d) - \bar{\mu}^1(d))]^2 - \frac{1}{N^2 p^2} \sum_{i=1}^N \text{E}^2 [Z_i (\mu_i(\mathbf{Y}(\mathbf{Z}); d) - \bar{\mu}^1(d))] \\
&\quad + \frac{1}{N^2 p^2} \sum_{i=1}^N \sum_{j \neq i}^N \text{Cov} [Z_i (\mu_i(\mathbf{Y}(\mathbf{Z}); d) - \bar{\mu}^1(d)), Z_j (\mu_j(\mathbf{Y}(\mathbf{Z}); d) - \bar{\mu}^1(d))] \\
&= \frac{1}{N^2 p} \sum_{i=1}^N \text{E} [\mu_i(\mathbf{Y}(1, \mathbf{Z}_{-i}); d) - \bar{\mu}^1(d)]^2 - \frac{1}{N^2} \sum_{i=1}^N \text{E}^2 [\mu_i(\mathbf{Y}(1, \mathbf{Z}_{-i}); d) - \bar{\mu}^1(d)] \\
&\quad + \frac{1}{N^2} \sum_{i=1}^N \sum_{j \neq i}^N \text{E} [(\mu_i(\mathbf{Y}(1, 1, \mathbf{Z}_{-(i,j)}); d) - \bar{\mu}^1(d)) (\mu_j(\mathbf{Y}(1, 1, \mathbf{Z}_{-(i,j)}); d) - \bar{\mu}^1(d))] \\
&\quad - \frac{1}{N^2} \sum_{i=1}^N \sum_{j \neq i}^N \text{E} [\mu_i(\mathbf{Y}(1, \mathbf{Z}_{-i}); d) - \bar{\mu}^1(d)] \text{E} [\mu_j(\mathbf{Y}(1, \mathbf{Z}_{-j}); d) - \bar{\mu}^1(d)] \\
&= \frac{1}{N^2 p} \sum_{i=1}^N \text{E} [\mu_i(\mathbf{Y}(1, \mathbf{Z}_{-i}); d) - \bar{\mu}^1(d)]^2 - \frac{1}{N^2} \sum_{i=1}^N \text{E}^2 [\mu_i(\mathbf{Y}(1, \mathbf{Z}_{-i}); d) - \bar{\mu}^1(d)] \\
&\quad + \frac{1}{N^2} \sum_{i=1}^N \sum_{j \in \mathcal{B}(i;d)} \text{E} [(\mu_i(\mathbf{Y}(1, 1, \mathbf{Z}_{-(i,j)}); d) - \bar{\mu}^1(d)) (\mu_j(\mathbf{Y}(1, 1, \mathbf{Z}_{-(i,j)}); d) - \bar{\mu}^1(d))] \\
&\quad - \frac{1}{N^2} \sum_{i=1}^N \sum_{j \in \mathcal{B}(i;d)} \text{E} [\mu_i(\mathbf{Y}(1, \mathbf{Z}_{-i}); d) - \bar{\mu}^1(d)] \text{E} [\mu_j(\mathbf{Y}(1, \mathbf{Z}_{-j}); d) - \bar{\mu}^1(d)].
\end{aligned}$$

Similarly, for the term $\text{Var} \left[\hat{\mu}^0(d) - \bar{\mu}^0(d) \hat{N}_1 \right]$, we have:

$$\begin{aligned}
& \text{Var} \left[\hat{\mu}^0(d) - \bar{\mu}^0(d) \hat{N}_0 \right] \\
&= \frac{1}{N^2(1-p)} \sum_{i=1}^N \text{E} \left[\mu_i(\mathbf{Y}(0, \mathbf{Z}_{-i}); d) - \bar{\mu}^0(d) \right]^2 - \frac{1}{N^2} \sum_{i=1}^N \text{E}^2 \left[\mu_i(\mathbf{Y}(0, \mathbf{Z}_{-i}); d) - \bar{\mu}^0(d) \right] \\
&+ \frac{1}{N^2} \sum_{i=1}^N \sum_{j \in \mathcal{B}(i;d)} \text{E} \left[(\mu_i(\mathbf{Y}(0, 0, \mathbf{Z}_{-(i,j)}); d) - \bar{\mu}^0(d)) (\mu_j(\mathbf{Y}(0, 0, \mathbf{Z}_{-(i,j)}); d) - \bar{\mu}^0(d)) \right] \\
&- \frac{1}{N^2} \sum_{i=1}^N \sum_{j \in \mathcal{B}(i;d)} \text{E} \left[\mu_i(\mathbf{Y}(0, \mathbf{Z}_{-i}); d) - \bar{\mu}^0(d) \right] \text{E} \left[\mu_j(\mathbf{Y}(0, \mathbf{Z}_{-j}); d) - \bar{\mu}^0(d) \right].
\end{aligned}$$

For the term $\text{Cov} \left[\hat{\mu}^1(d) - \bar{\mu}^1(d) \hat{N}_1, \hat{\mu}^0(d) - \bar{\mu}^0(d) \hat{N}_0 \right]$, we have

$$\begin{aligned}
& \text{Cov} \left[\hat{\mu}^1(d) - \bar{\mu}^1(d) \hat{N}_1, \hat{\mu}^0(d) - \bar{\mu}^0(d) \hat{N}_0 \right] \\
&= \frac{1}{N^2 p(1-p)} \text{Cov} \left[\sum_{i=1}^N Z_i (\mu_i(\mathbf{Y}(\mathbf{Z}); d) - \bar{\mu}^1(d)), \sum_{j=1}^N (1 - Z_j) (\mu_j(\mathbf{Y}(\mathbf{Z}); d) - \bar{\mu}^0(d)) \right] \\
&= \frac{1}{N^2} \sum_{i=1}^N \sum_{j \neq i}^N \text{E} \left[(\mu_i(\mathbf{Y}(1, 0, \mathbf{Z}_{-(i,j)}); d) - \bar{\mu}^1(d)) (\mu_j(\mathbf{Y}(1, 0, \mathbf{Z}_{-(i,j)}); d) - \bar{\mu}^0(d)) \right] \\
&- \frac{1}{N^2} \sum_{i=1}^N \sum_{j \neq i}^N \text{E} \left[\mu_i(\mathbf{Y}(1, \mathbf{Z}_{-i}); d) - \bar{\mu}^1(d) \right] \text{E} \left[\mu_j(\mathbf{Y}(0, \mathbf{Z}_{-j}); d) - \bar{\mu}^0(d) \right] \\
&= \frac{1}{N^2} \sum_{i=1}^N \sum_{j \in \mathcal{B}(i;d)} \text{E} \left[(\mu_i(\mathbf{Y}(1, 0, \mathbf{Z}_{-(i,j)}); d) - \bar{\mu}^1(d)) (\mu_j(\mathbf{Y}(1, 0, \mathbf{Z}_{-(i,j)}); d) - \bar{\mu}^0(d)) \right] \\
&- \frac{1}{N^2} \sum_{i=1}^N \sum_{j \in \mathcal{B}(i;d)} \text{E} \left[\mu_i(\mathbf{Y}(1, \mathbf{Z}_{-i}); d) - \bar{\mu}^1(d) \right] \text{E} \left[\mu_j(\mathbf{Y}(0, \mathbf{Z}_{-j}); d) - \bar{\mu}^0(d) \right]
\end{aligned}$$

Combining these terms leads to the variance expression in (3). Note that for the last term

in the expression, we have

$$\begin{aligned}
& \frac{1}{N} \sum_{i=1}^N \sum_{j \in \mathcal{B}(i;d)} \sum_{a,b=0}^1 (-1)^{a+b} \mathbb{E} [\mu_i(\mathbf{Y}(a, \mathbf{Z}_{-i}); d) - \bar{\mu}^a(d)] \mathbb{E} [\mu_j(\mathbf{Y}(b, \mathbf{Z}_{-j}); d) - \bar{\mu}^b(d)] \\
&= \frac{1}{N} \sum_{i=1}^N \sum_{j \in \mathcal{B}(i;d)} \left\{ \mathbb{E} [\mu_i(\mathbf{Y}(1, \mathbf{Z}_{-i}); d) - \bar{\mu}^1(d)] \right. \\
&\quad \times \mathbb{E} [\mu_j(\mathbf{Y}(1, \mathbf{Z}_{-j}); d) - \mu_j(\mathbf{Y}(0, \mathbf{Z}_{-j}); d) - (\bar{\mu}^1(d) - \bar{\mu}^0(d))] \left. \right\} \\
&\quad - \frac{1}{N} \sum_{i=1}^N \sum_{j \in \mathcal{B}(i;d)} \left\{ \mathbb{E} [\mu_j(\mathbf{Y}(0, \mathbf{Z}_{-j}); d) - \bar{\mu}^0(d)] \right. \\
&\quad \times \mathbb{E} [\mu_i(\mathbf{Y}(1, \mathbf{Z}_{-i}); d) - \mu_i(\mathbf{Y}(0, \mathbf{Z}_{-i}); d) - (\bar{\mu}^1(d) - \bar{\mu}^0(d))] \left. \right\} \\
&= \frac{1}{N} \sum_{i=1}^N (\tau_i(d; \eta) - \tau(d; \eta)) \sum_{j \in \mathcal{B}(i;d)} (\tau_j(d; \eta) - \tau(d; \eta)).
\end{aligned}$$

where $\tau_i(d; \eta)$, $\tau_j(d; \eta)$ and $\tau(d; \eta)$ are defined as in C5. Clearly the expression of interest is smaller than or equal to zero in the limit under C5, which proves the lemma. From lemma A.3, we know that $\Pr(N\text{Var}(\hat{\tau}_{HA}(d)) \leq N\tilde{V}) \rightarrow 1$. \square

A.3 Propositions 2 and 3 (Asymptotic Distributions)

The consistency of the proposed estimator follows from the fact that both $\text{Var}(\hat{\tau}(d))$ and $\text{Var}(\hat{\tau}_{HA}(d))$ converge to zero as $N \rightarrow \infty$ under conditions C1-C4. The asymptotic normality of the Horvitz-Thompson estimator can be derived using classic central limit theorems for dependent random variables based on Stein's method (Ross et al., 2011; Ogburn et al., 2020). The Hajek estimator's asymptotic distribution can be then obtained via the Delta method. We first restate the key lemmas in Ogburn et al. (2020) using terms defined in this paper.

Lemma A.5. (Ogburn et al. (2020), Lemma 1 and 2) Consider a set of N units. Let U_1, \dots, U_N be bounded mean-zero random variables with finite fourth moments and depen-

density neighborhoods $\mathcal{B}(i; d)$. If $c_i(d) \leq \tilde{c}$ for all i and $\tilde{c}^2/N \rightarrow 0$, then

$$\frac{\sum_{i=1}^N U_i}{\sqrt{\text{Var}(\sum_{i=1}^N U_i)}} \rightarrow N(0, 1).$$

Now we can prove propositions 2 and 3 using the above lemma.

Propositions 2 and 3 (asymptotic normality of $\hat{\tau}(d)$ and $\hat{\tau}_{HA}(d)$).

Proof. Define U_i as $\sqrt{N} \left(\frac{Z_i \mu_i(\mathbf{Y}(1, \mathbf{Z}_{-i}); d)}{Np} - \frac{(1-Z_i) \mu_i(\mathbf{Y}(0, \mathbf{Z}_{-i}); d)}{N(1-p)} - \frac{\text{E}[\mu_i(\mathbf{Y}(1, \mathbf{Z}_{-i}); d)] - \text{E}[\mu_i(\mathbf{Y}(0, \mathbf{Z}_{-i}); d)]}{N} \right)$. Then, $\sum_{i=1}^N U_i = \sqrt{N}(\hat{\tau}(d) - \tau(d; \eta))$ and $\text{E}[U_i] = 0$. We know that U_i has finite fourth moments and $\text{Var}(\sum_{i=1}^N U_i) = N \text{Var}(\hat{\tau}(d))$ is also finite. By condition C 4a, $c_i(d) \leq \tilde{c}$ in our case and $\tilde{c}^2/N \rightarrow 0$. From Lemma A.5, we know that $\frac{\sqrt{N}(\hat{\tau}(d) - \tau(d; \eta))}{\sqrt{\text{Var}[\sqrt{N}(\hat{\tau}(d) - \tau(d; \eta))]}} \rightarrow N(0, 1)$ and $\sqrt{N}(\hat{\tau}(d) - \tau(d; \eta)) \rightarrow N(0, V_{HT})$. It is easy to show that $\sqrt{N}(\tilde{N}_1 - 1) \rightarrow N(0, \frac{1-p}{p})$ and $\sqrt{N}(\tilde{N}_0 - 1) \rightarrow N(0, \frac{p}{1-p})$. In the proof of lemma A.3, we have seen that $\sqrt{N}(\hat{\tau}_{HA}(d) - \tau(d; \eta)) = \sqrt{N}(\hat{\tau}(d) - \tau(d; \eta)) + \sqrt{N}\bar{\mu}^0(d)(\tilde{N}_1 - 1) + \sqrt{N}\bar{\mu}^1(d)(\tilde{N}_0 - 1) + o_P(1)$. Therefore, $\sqrt{N}(\hat{\tau}_{HA}(d) - \tau(d; \eta))$ converges to a normal distribution as well. \square

A.4 Estimation with regression and spatial HAC standard error

Our estimation of $\tau(d; \eta)$ could be seen as a two-step process. In the first step, we construct the circle average for each intervention node: $\mu_i(d) \stackrel{def}{=} \mu_i(\mathbf{Y}(\mathbf{Z}); d) = \frac{\sum_x \mathbf{1}\{d_{ix}=d\} Y_x}{\sum_x \mathbf{1}\{d_{ix}=d\}}$. In the second step, we apply the Horvitz-Thompson estimator or the Hajek estimator to all the $(Z_i, \mu_i(d))$. As we focus on bipartite designs (Zigler and Papadogeorgou, 2018), it is convenient to assume that $|\mathcal{X}| \gg N$ hence uncertainties in the first step can be ignored.

Treating $\mu_i(d)$ as the outcome variable, we estimate the following regression equation:

$$\mu_i(d) = a(d) + \tau(d)Z_i + \varepsilon_i(d).$$

Estimating this regression model with ordinary least squares (OLS), $\hat{a}(d) = \frac{1}{N_0} \sum_{i=1}^N (1 -$

$Z_i)\mu_i(d) \stackrel{def}{=} \hat{\mu}^0(d)$ and $\hat{\tau}_{OLS}(d) = \frac{1}{N_1} \sum_{i=1}^N Z_i \mu_i(d) - \frac{1}{N_0} \sum_{i=1}^N (1 - Z_i) \mu_i(d) = \hat{\mu}^1(d) - \hat{\mu}^0(d)$.

Clearly, $\hat{\tau}_{OLS}(d) = \hat{\tau}_{HA}(d)$. Then the residual for each observation is $\hat{e}_i(d) = \mu_i(d) - \hat{a}(d) - \hat{\tau}_{OLS}(d)Z_i = \mu_i(d) - \hat{\mu}^0(d) - [\hat{\mu}^1(d) - \hat{\mu}^0(d)]Z_i$.

Denoting $\begin{pmatrix} 1, Z_1 \\ 1, Z_2 \\ \dots \\ 1, Z_N \end{pmatrix}$ as \mathbf{X} , [Conley \(1999\)](#)'s spatial HAC standard errors of $(\hat{a}(d), \hat{\tau}_{OLS}(d))$

can be expressed as:

$$\begin{aligned} \sigma \begin{pmatrix} \hat{a}(d) \\ \hat{\tau}_{OLS}(d) \end{pmatrix} &= \sqrt{\text{Var} \begin{pmatrix} \hat{a}(d) \\ \hat{\tau}_{OLS}(d) \end{pmatrix}} \\ \widehat{\text{Var}} \begin{pmatrix} \hat{a}(d) \\ \hat{\tau}_{OLS}(d) \end{pmatrix} &= (\mathbf{X}'\mathbf{X})^{-1}(\mathbf{X}'\Sigma\mathbf{X})(\mathbf{X}'\mathbf{X})^{-1} \\ &= \begin{pmatrix} N, N_1 \\ N_1, N_1 \end{pmatrix}^{-1} \left(\sum_{i=1}^N \sum_{j=1}^N \mathbf{X}_i \mathbf{X}_j' \hat{e}_i(d) \hat{e}_j(d) \mathbf{1}\{j \in \mathcal{B}(i; d)\} \right) \begin{pmatrix} N, N_1 \\ N_1, N_1 \end{pmatrix}^{-1} \\ &= \frac{1}{N_1^2 N_0^2} \begin{pmatrix} N_1, -N_1 \\ -N_1, N \end{pmatrix} \left(\sum_{i=1}^N \sum_{j=1}^N \begin{pmatrix} 1, Z_j \\ Z_i, Z_i Z_j \end{pmatrix} \hat{e}_i(d) \hat{e}_j(d) \mathbf{1}\{j \in \mathcal{B}(i; d)\} \right) \begin{pmatrix} N_1, -N_1 \\ -N_1, N \end{pmatrix}. \end{aligned}$$

Note that the (2, 2) entry of $\begin{pmatrix} N_1, -N_1 \\ -N_1, N \end{pmatrix} \begin{pmatrix} 1, Z_j \\ Z_i, Z_i Z_j \end{pmatrix} \begin{pmatrix} N_1, -N_1 \\ -N_1, N \end{pmatrix}$ equals to $N_1^2 - N_1 N Z_i - N_1 N Z_j + N^2 Z_i Z_j$. Rearrange the sample such that treated observations lie before obser-

variations under control and plug in the expression of $\hat{e}_i(d)$, we can see that:

$$\begin{aligned}
& \widehat{\text{Var}}(\hat{\tau}_{OLS}(d)) \\
&= \frac{1}{N_1^2} \sum_{i=1}^{N_1} \hat{e}_i^2(d) + \frac{1}{N_0^2} \sum_{i=N_1+1}^N \hat{e}_i^2(d) + \frac{1}{N_1^2} \sum_{i=1}^{N_1} \sum_{j \neq i, Z_j=1} \hat{e}_i(d) \hat{e}_j(d) - \frac{1}{N_1 N_0} \sum_{i=1}^{N_1} \sum_{j \neq i, Z_j=0} \hat{e}_i(d) \hat{e}_j(d) \\
&\quad - \frac{1}{N_1 N_0} \sum_{i=N_1+1}^N \sum_{j \neq i, Z_j=1} \hat{e}_i(d) \hat{e}_j(d) + \frac{1}{N_0^2} \sum_{i=N_1+1}^N \sum_{j \neq i, Z_j=0} \hat{e}_i(d) \hat{e}_j(d) \\
&= \underbrace{\frac{1}{N_1^2} \sum_{i=1}^{N_1} (\mu_i(d) - \hat{\mu}^1(d))^2}_{(A)} + \underbrace{\frac{1}{N_0^2} \sum_{i=N_1+1}^N (\mu_i(d) - \hat{\mu}^0(d))^2}_{(B)} \\
&\quad + \underbrace{\frac{1}{N_1^2} \sum_{i=1}^{N_1} \sum_{j \in \mathcal{B}(i;d), Z_j=1} (\mu_i(d) - \hat{\mu}^1(d)) (\mu_j(d) - \hat{\mu}^1(d))}_{(C)} \\
&\quad - \underbrace{\frac{1}{N_1 N_0} \sum_{i=1}^{N_1} \sum_{j \in \mathcal{B}(i;d), Z_j=0} (\mu_i(d) - \hat{\mu}^1(d)) (\mu_j(d) - \hat{\mu}^0(d))}_{(D)} \\
&\quad - \underbrace{\frac{1}{N_1 N_0} \sum_{i=N_1+1}^N \sum_{j \in \mathcal{B}(i;d), Z_j=1} (\mu_i(d) - \hat{\mu}^0(d)) (\mu_j(d) - \hat{\mu}^1(d))}_{(E)} \\
&\quad + \underbrace{\frac{1}{N_0^2} \sum_{i=N_1+1}^N \sum_{j \in \mathcal{B}(i;d), Z_j=0} (\mu_i(d) - \hat{\mu}^0(d)) (\mu_j(d) - \hat{\mu}^0(d))}_{(F)}
\end{aligned}$$

Finally, we show that the variance estimate $N \widehat{\text{Var}}(\hat{\tau}_{OLS}(d))$ is consistent for the rescaled variance bound defined in Lemma A.4, $N \tilde{V}$. As we have seen, $N \tilde{V}$ is an upwardly biased estimate of the true variance of the linearized Hajek estimator. The normal confidence interval with the OLS variance estimates therefore provides conservative coverage for the Hajek estimator asymptotically.

Lemma A.6.

$$N\widehat{\text{Var}}(\hat{\tau}_{OLS}(d)) - N\bar{V} \xrightarrow{p} 0$$

Proof. We first establish the limit of (A).

$$\begin{aligned} & N \left[\frac{1}{N_1^2} \sum_{i=1}^{N_1} (\mu_i(\mathbf{Y}(\mathbf{Z}); d) - \hat{\mu}^1(d))^2 \right] \\ &= N \left[\frac{1}{N_1^2} \sum_{i=1}^{N_1} \mu_i^2(\mathbf{Y}(\mathbf{Z}); d) - \frac{1}{N_1} (\hat{\mu}^1(d))^2 \right] \\ &= p \frac{N^2}{N_1^2} \frac{1}{Np} \sum_{i=1}^{N_1} \mu_i^2(\mathbf{Y}(\mathbf{Z}); d) - \frac{N}{N_1} (\hat{\mu}^1(d))^2 \\ &\xrightarrow{p} \frac{1}{p} \times \frac{1}{N} \sum_{i=1}^N E[\mu_i^2(\mathbf{Y}(1, \mathbf{Z}_{-i}), d)] - \frac{1}{p} (\bar{\mu}^1(d))^2 \\ &= \frac{1}{p} \frac{1}{N} \sum_{i=1}^N E[(\mu_i(\mathbf{Y}(1, \mathbf{Z}_{-i}), d) - \bar{\mu}^1(d))^2]. \end{aligned}$$

The convergence in probability is justified by noting $\frac{1}{Np} \sum_{i=1}^{N_1} \mu_i^2(\mathbf{Y}(\mathbf{Z}); d)$ and $\frac{1}{Np} N_1$ are both Horvitz-Thompson estimators, and under C1-C3 they converge to their mean in probability.

(B) can be established in a similar manner.

Now consider (C), we have:

$$\begin{aligned}
& N \frac{1}{N_1^2} \sum_{i=1}^{N_1} \sum_{j \in \mathcal{B}(i;d), Z_j=1} (\mu_i(\mathbf{Y}(\mathbf{Z}); d) - \hat{\mu}^1(d)) (\mu_j(\mathbf{Y}(\mathbf{Z}); d) - \hat{\mu}^1(d)) \\
&= N \frac{1}{N_1^2} \sum_{i=1}^N \sum_{j \in \mathcal{B}(i;d)} Z_i Z_j (\mu_i(\mathbf{Y}(\mathbf{Z}); d) - \bar{\mu}^1(d)) (\mu_j(\mathbf{Y}(\mathbf{Z}); d) - \bar{\mu}^1(d)) \\
&\quad + \frac{N}{N_1^2} \sum_{i=1}^N \sum_{j \in \mathcal{B}(i;d)} Z_i Z_j (\bar{\mu}^1(d) - \hat{\mu}^1(d)) (\mu_j(\mathbf{Y}(\mathbf{Z}); d) - \hat{\mu}^1(d)) \\
&\quad + \frac{N}{N_1^2} \sum_{i=1}^N \sum_{j \in \mathcal{B}(i;d)} Z_i Z_j (\mu_i(\mathbf{Y}(\mathbf{Z}) - \hat{\mu}^1(d)) (\bar{\mu}^1(d) - \hat{\mu}^1(d)) \\
&= \frac{N^2}{N_1^2} \frac{1}{N} \sum_{i=1}^N \sum_{j \in \mathcal{B}(i;d)} Z_i Z_j (\mu_i(\mathbf{Y}(\mathbf{Z}); d) - \bar{\mu}^1(d)) (\mu_j(\mathbf{Y}(\mathbf{Z}); d) - \bar{\mu}^1(d)) \\
&\quad + \frac{N^2}{N_1^2} \frac{1}{N} \sum_{i=1}^N \sum_{j \in \mathcal{B}(i;d)} Z_i Z_j (\mu^1(d) - \hat{\mu}^1(d)) (\mu_j(\mathbf{Y}(\mathbf{Z}); d) - \hat{\mu}^1(d)) \\
&\quad + \frac{N^2}{N_1^2} \frac{1}{N} \sum_{i=1}^N \sum_{j \in \mathcal{B}(i;d)} Z_i Z_j (\mu_i(\mathbf{Y}(\mathbf{Z}) - \hat{\mu}^1(d)) (\mu^1(d) - \hat{\mu}^1(d)) \\
&\stackrel{p}{\rightarrow} \frac{1}{N} \sum_{i=1}^N \sum_{j \in \mathcal{B}(i;d)} \text{E} [(\mu_i(\mathbf{Y}(1, 1, \mathbf{Z}_{-(i,j)}); d) - \bar{\mu}^1(d)) (\mu_j(\mathbf{Y}(1, 1, \mathbf{Z}_{-(i,j)}); d) - \bar{\mu}^1(d))]
\end{aligned}$$

For the last line we use the fact that:

1. The second and third terms are of order $o_p(1)$. For the second term, for example,

$$\begin{aligned}
& \left| \frac{N^2}{N_1^2} (\bar{\mu}^1(d) - \hat{\mu}^1(d)) \frac{1}{N} \sum_{i=1}^N \sum_{j \in \mathcal{B}(i;d)} Z_i Z_j (\mu_i(\mathbf{Y}(\mathbf{Z}) - \hat{\mu}^1(d)) \right| \\
&\leq \frac{N^2}{N_1^2} |\bar{\mu}^1(d) - \hat{\mu}^1(d)| \times \frac{1}{N} \sum_{i=1}^N d_i |\mu_i(\mathbf{Y}(\mathbf{Z}) - \hat{\mu}^1(d)| \\
&= o_p(1) \times O_p(1) = o_p(1)
\end{aligned}$$

where d_i is i 's degree in the dependency graph. The argument is the same for the third

term.

2. For the convergence of the first term, the argument is the same as in Proposition 6.2 in [Aronow and Samii \(2017\)](#).

□

A.5 An alternative variance estimator

In the previous section, we discussed the inference procedure for the Hajek estimator under [C5](#). We now provide an alternative approach, based on a proposal in [Sävje et al. \(2021\)](#). We have the following lemma:

Lemma A.7. *Under [C1-C4](#), we have*

$$\begin{aligned} \text{Var}(\hat{\tau}_{HA}^{Taylor}(d)) &\leq \bar{V}(d) \\ &= \frac{1}{N^2} \sum_{i=1}^N c_i(d) \frac{\text{E}[\mu_i(\mathbf{Y}(1, \mathbf{Z}_{-i}), d) - \bar{\mu}^1(d)]^2}{p} + \frac{1}{N^2} \sum_{i=1}^N c_i(d) \frac{\text{E}[\mu_i(\mathbf{Y}(0, \mathbf{Z}_{-i}), d) - \bar{\mu}^0(d)]^2}{1-p}. \end{aligned}$$

The estimator $\hat{V}(d)$

$$\hat{V}(d) = \frac{1}{N^2} \sum_{i=1}^N Z_i c_i(d) \frac{(\mu_i(\mathbf{Z}, d) - \hat{\mu}^1(d))^2}{p^2} + \frac{1}{N^2} \sum_{i=1}^N (1 - Z_i) c_i(d) \frac{(\mu_i(\mathbf{Z}, d) - \hat{\mu}^0(d))^2}{(1-p)^2}$$

is consistent for $\bar{V}(d)$: $N\hat{V}(d) - N\bar{V}(d) \xrightarrow{P} 0$.

Proof. The proof is built upon the following inequalities:

$$\begin{aligned} &\text{Var} \left[\frac{Z_i(\mu_i(\mathbf{Y}(\mathbf{Z}), d) - \mu^1(d))}{p} - \frac{(1 - Z_i)(\mu_i(\mathbf{Y}(\mathbf{Z}), d) - \mu^0(d))}{1-p} \right] \\ &\leq \frac{\text{E}[\mu_i(\mathbf{Y}(1, \mathbf{Z}_{-i}), d) - \mu^1(d)]^2}{p} + \frac{\text{E}[\mu_i(\mathbf{Y}(0, \mathbf{Z}_{-i}), d) - \mu^0(d)]^2}{1-p}, \\ &\text{Cov}[A_i, A_j] \leq \frac{\text{Var}[A_i] + \text{Var}[A_j]}{2}. \end{aligned}$$

Let's define $A_i = \frac{Z_i(\mu_i(\mathbf{Y}(\mathbf{Z}),d) - \mu^1(d))}{p}$ and $B_i = \frac{(1-Z_i)(\mu_i(\mathbf{Y}(\mathbf{Z}),d) - \mu^0(d))}{1-p}$, then

$$\begin{aligned}
\text{Var} \left[\hat{\tau}_{HA}^{Taylor} \right] &= \frac{1}{N^2} \sum_{i=1}^N \text{Var} [A_i - B_i] + \frac{1}{N^2} \sum_{i=1}^N \sum_{j \neq i} \text{Cov} [A_i - B_i, A_j - B_j] \\
&= \frac{1}{N^2} \sum_{i=1}^N \text{Var} [A_i - B_i] + \frac{1}{N^2} \sum_{i=1}^N \sum_{j \in \mathcal{B}(i;d)} \text{Cov} [A_i - B_i, A_j - B_j] \\
&\leq \frac{1}{N^2} \sum_{i=1}^N \text{Var} [A_i - B_i] + \frac{1}{N^2} \sum_{i=1}^N \sum_{j \in \mathcal{B}(i;d)} \frac{\text{Var} [A_i - B_i] + \text{Var} [A_j - B_j]}{2} \\
&= \frac{1}{N^2} \sum_{i=1}^N \text{Var} [A_i - B_i] + \frac{1}{N^2} \sum_{i=1}^N c_i(d) \text{Var} [A_i - B_i].
\end{aligned}$$

Then, we just apply the first inequality. The proof for the consistency of the estimator is straightforward hence omitted. \square

A.6 Effective degree of freedom adjustment

Consider the following regression representation of the Hajek estimator:

$$\mu_i(d) = a(d) + \tau(d)Z_i + \varepsilon_i(d).$$

It has the following matrix form:

$$\mu(d) = \mathbf{X} \begin{pmatrix} a(d) \\ \tau(d) \end{pmatrix} + \varepsilon(d).$$

where $\mu(d) = \begin{pmatrix} \mu_1(d) \\ \mu_2(d) \\ \vdots \\ \mu_N(d) \end{pmatrix}$, $\varepsilon(d) = \begin{pmatrix} \varepsilon_1(d) \\ \varepsilon_2(d) \\ \vdots \\ \varepsilon_N(d) \end{pmatrix}$, and \mathbf{X} is defined as above in the main text.

Suppose we want to test the null hypothesis $\tau(d) = \tau_0$, which can be expressed as $\mathbf{w}' \begin{pmatrix} a(d) \\ \tau(d) \end{pmatrix} = \tau_0$ with $\mathbf{w}' = (0, 1)$. Under a working model that assumes $\varepsilon_i(d) \sim N(0, \sigma^2)$, the t-statistic under the null can be written as

$$\frac{\hat{\tau}(d) - \tau_0}{\sqrt{\mathbf{w}' \hat{\mathbf{V}} \mathbf{w}}} = \frac{\frac{\hat{\tau}(d) - \tau_0}{\sqrt{\sigma^2 \mathbf{w}' (\mathbf{X}' \mathbf{X})^{-1} \mathbf{w}}}}{\sqrt{\frac{\mathbf{w}' \hat{\mathbf{V}} \mathbf{w}}{\sigma^2 \mathbf{w}' (\mathbf{X}' \mathbf{X})^{-1} \mathbf{w}}}},$$

where $\hat{\mathbf{V}}$ is an estimate of the variance of $\begin{pmatrix} \hat{a}(d) \\ \hat{\tau}(d) \end{pmatrix}$. We expect the statistic to converge to the t-distribution. As the numerator converges to the standard normal distribution according to the central limit theorem, all we need is that the square of the denominator converges to the chi-square distribution.

Young (2015) notes that for most variance estimators, the square of the denominator (which is a random scalar) can be further written as a quadratic form of the error term $\varepsilon(d)$:

$$\frac{\mathbf{w}' \hat{\mathbf{V}} \mathbf{w}}{\sigma^2 \mathbf{w}' (\mathbf{X}' \mathbf{X})^{-1} \mathbf{w}} = \frac{\varepsilon(d)'}{\sigma} \mathbf{B} \frac{\varepsilon(d)}{\sigma}.$$

As $\frac{\varepsilon(d)}{\sigma}$ is normally distributed, the quantity obeys the chi-square distribution in finite samples if \mathbf{B} equals the identity matrix \mathbf{I} . Otherwise, as Young (2015) proposes, we should adjust $\hat{\mathbf{V}}$ via dividing it by $\eta = \text{trace}(\mathbf{B})$. After this effective degree of freedom adjustment, the quantity's variance will be twice as large as its expectation, which is a property satisfied

by the chi-square distribution. In other words, the distribution of the adjusted t-statistic will be a closer approximation of the t-distribution. The argument holds even if $\varepsilon(d)$ is not normally distributed.

Define $\lambda = \mathbf{w}'(\mathbf{X}'\mathbf{X})^{-1}\mathbf{X} = (\lambda_1, \lambda_2, \dots, \lambda_N)$ and $\mathbf{M} = \mathbf{I} - \mathbf{X}'(\mathbf{X}'\mathbf{X})^{-1}\mathbf{X}$. When $\hat{\mathbf{V}}$ is estimated via the spatial HAC variance estimator, we have

$$\mathbf{B} = \frac{N_1 N_0}{N} \mathbf{M} \left(\sum_{i=1}^N \sum_{j=1}^N \lambda_i \lambda_j \mathbf{1}\{j \in \mathcal{B}(i; d)\} \right) \mathbf{M}.$$

Therefore, with the effective degree of freedom adjustment, our variance estimate become $\frac{\hat{\mathbf{V}}}{\eta}$, where $\eta = \text{trace}(\mathbf{B})$.

B Extra results

B.1 DGP in the simulation

In the simulation, we first generate a raster with $80 \times 80 = 6,400$ tiles, each of which is an outcome point. The untreated potential outcome for outcome point x , $Y_x(0)$, is randomly drawn from the standard normal distribution. For point interventions, we divide the raster equally into 64 areas, take the centroid of each area, disturb their positions slightly (using the *jitter* function in R), and use these disturbed centroids as the positions of the intervention nodes. For polygon interventions, we aggregate the raster to a larger raster with 640 tiles, implement Voronoi tessellation on the larger raster to generate polygons, and randomly sample 64 polygons from the set.

We consider two effect functions. The first one is non-monotonic and additive. For an outcome point x which is d away from an intervention node i , the effect on it emanating from i equals:

$$f_x(d) = \alpha_x [\Gamma(d; 1, 1) - \Gamma(d; 5, 0.5)],$$

where $\Gamma(d; a, b)$ is the value of a Gamma distribution with shape a and scale b at d ; α_x captures the heterogeneity in the treatment effects on x . α_x are generated from kriging interpolation of 16 randomly drawn values. The treated potential outcome for outcome point x , $Y_x(\mathbf{Z})$, equals

$$Y_x(\mathbf{Z}) = Y_x(0) + \sum_{i=1}^{64} f_x(d_{ix}) * Z_i,$$

where $Z_i \sim \text{Bernoulli}(0.5)$. The second effect function is interactive. $f_x(d)$ is as before when one of x 's neighbors is untreated and equals $\alpha_x \Gamma(d; 1, 1)$, a monotonic function of d , when the same neighbor is treated.

To obtain of the values of the AME, we re-assign \mathbf{Z} for 1,000 times. Denote the p th

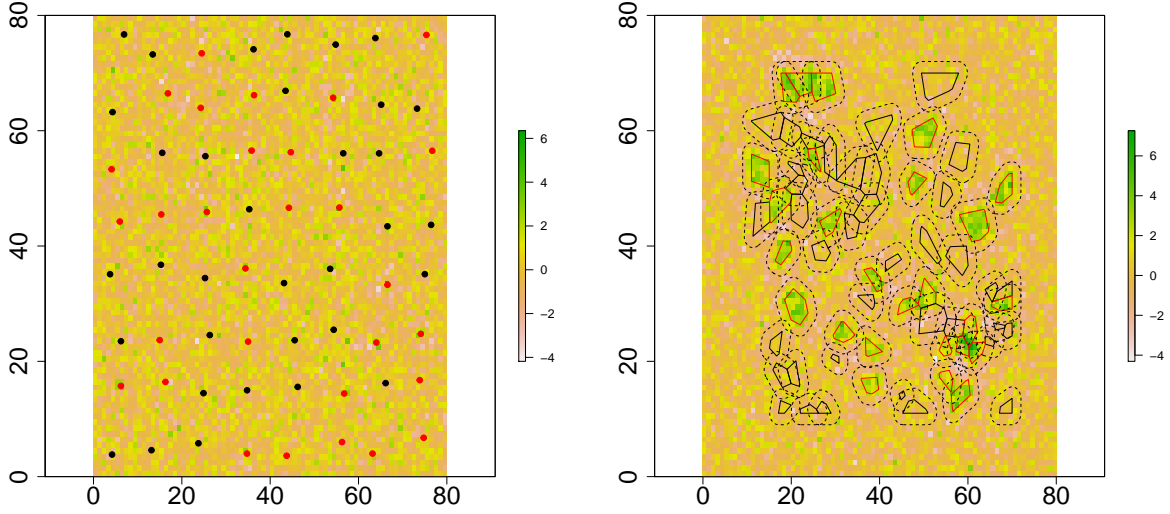


Figure 10: The plots show the structure of data in our simulation. On the left is a point intervention. Each treated point is marked in red and each untreated one is marked in black. Colors in the background indicate the outcome values. On the right is a polygon intervention. Treated and untreated nodes are marked by red and black borders, respectively. It also demonstrates buffers around each intervention polygon.

assignment of \mathbf{Z} as \mathbf{Z}_p and the value of Z_i under the assignment as Z_{pi} , then

$$\tau_{ix}(\eta) \approx \frac{\sum_{p=1}^{1000} Z_{pi} Y_x(\mathbf{Z}_p)}{\sum_{p=1}^{1000} Z_{pi}} - \frac{\sum_{p=1}^{1000} (1 - Z_{pi}) Y_x(\mathbf{Z}_p)}{\sum_{p=1}^{1000} 1 - Z_{pi}}.$$

$\tau_i(d; \eta)$ and $\tau(d; \eta)$ can be constructed following their definitions.

B.2 Extra results from simulation

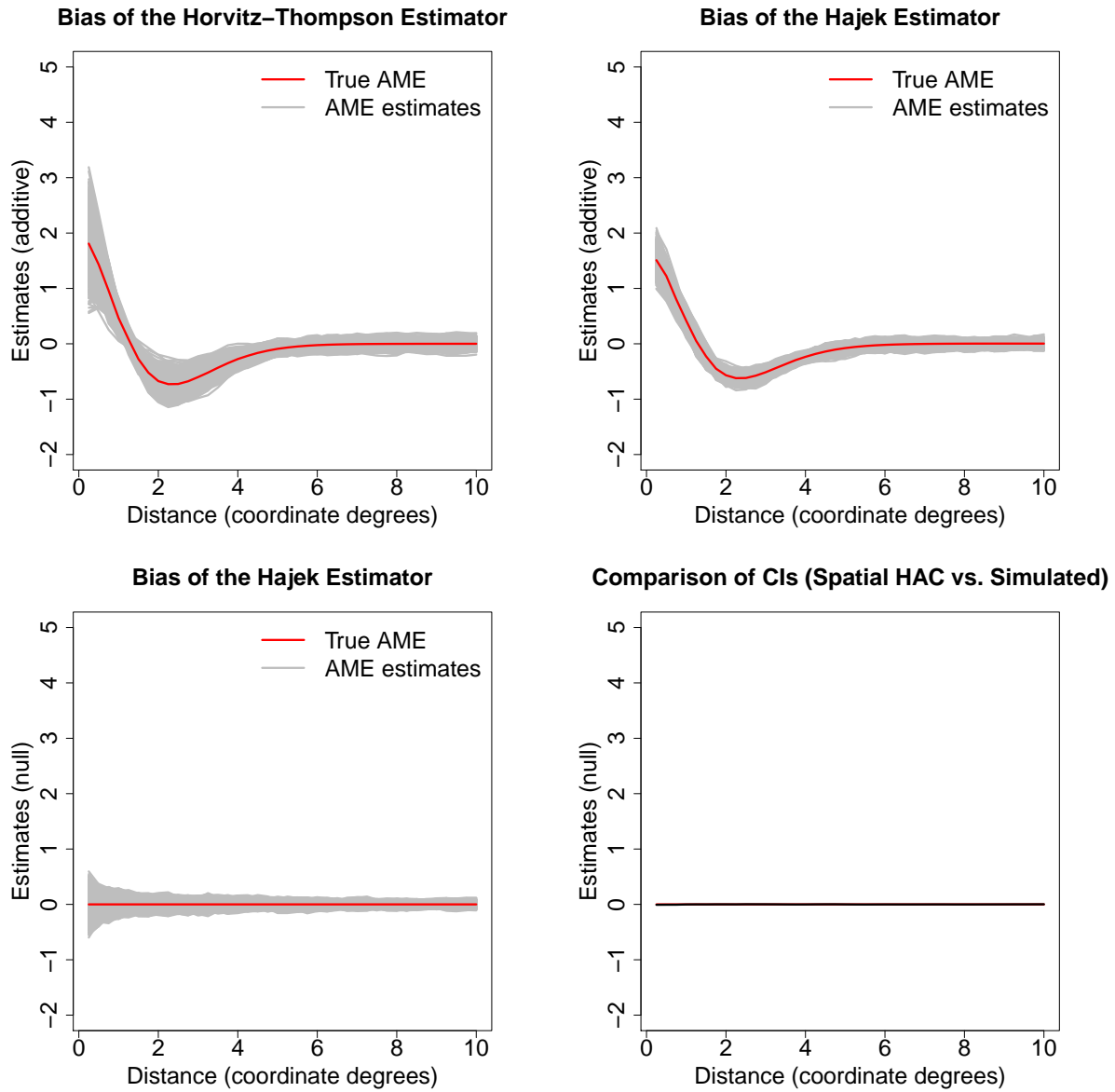


Figure 11: The top-left plot shows the bias of the Horvitz-Thompson estimator in the Bernoulli point intervention. The top-right plot shows the bias of the Hajek estimator in a point intervention where the treatment is assigned following complete randomization. The bottom-right plot shows the bias of the Hajek estimator in the Bernoulli point intervention, when the effect function equals zero across all the distance values. The red curves indicate the true AME curve and each grey curve represents the estimates under one random assignment. The bottom-right plot compares the simulated 95% confidence intervals with the averages of 95% Spatial HAC confidence intervals under the null effect function.

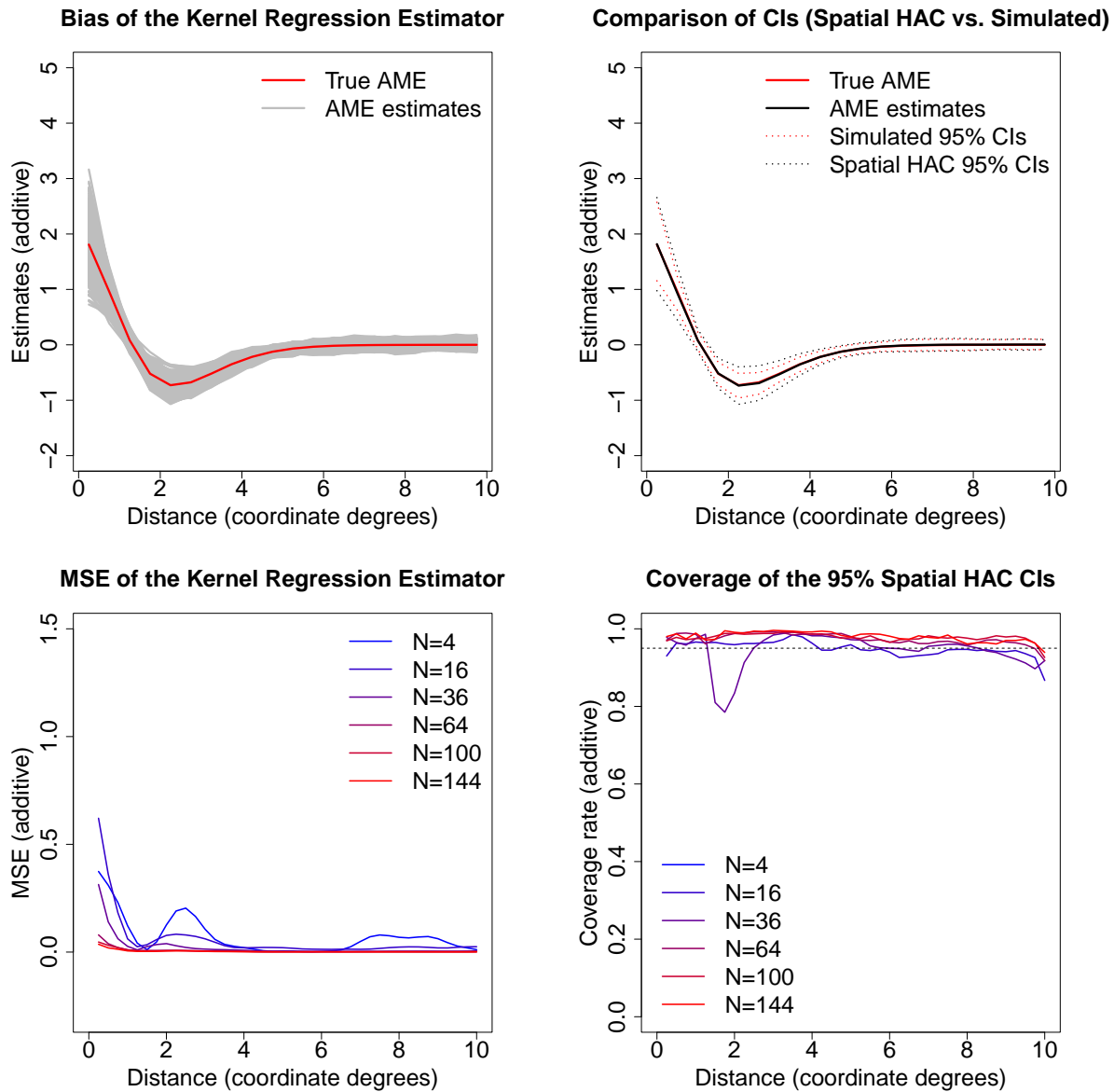


Figure 12: These plots show results from the kernel regression estimator in the Bernoulli point intervention. The top-left plot presents the bias of the estimator. The top-right plot compares the simulated 95% confidence intervals with the averages of 95% Spatial HAC confidence intervals. The two plots on the bottom demonstrate how the MSE and the coverage rate of the estimator varies with sample sizes.

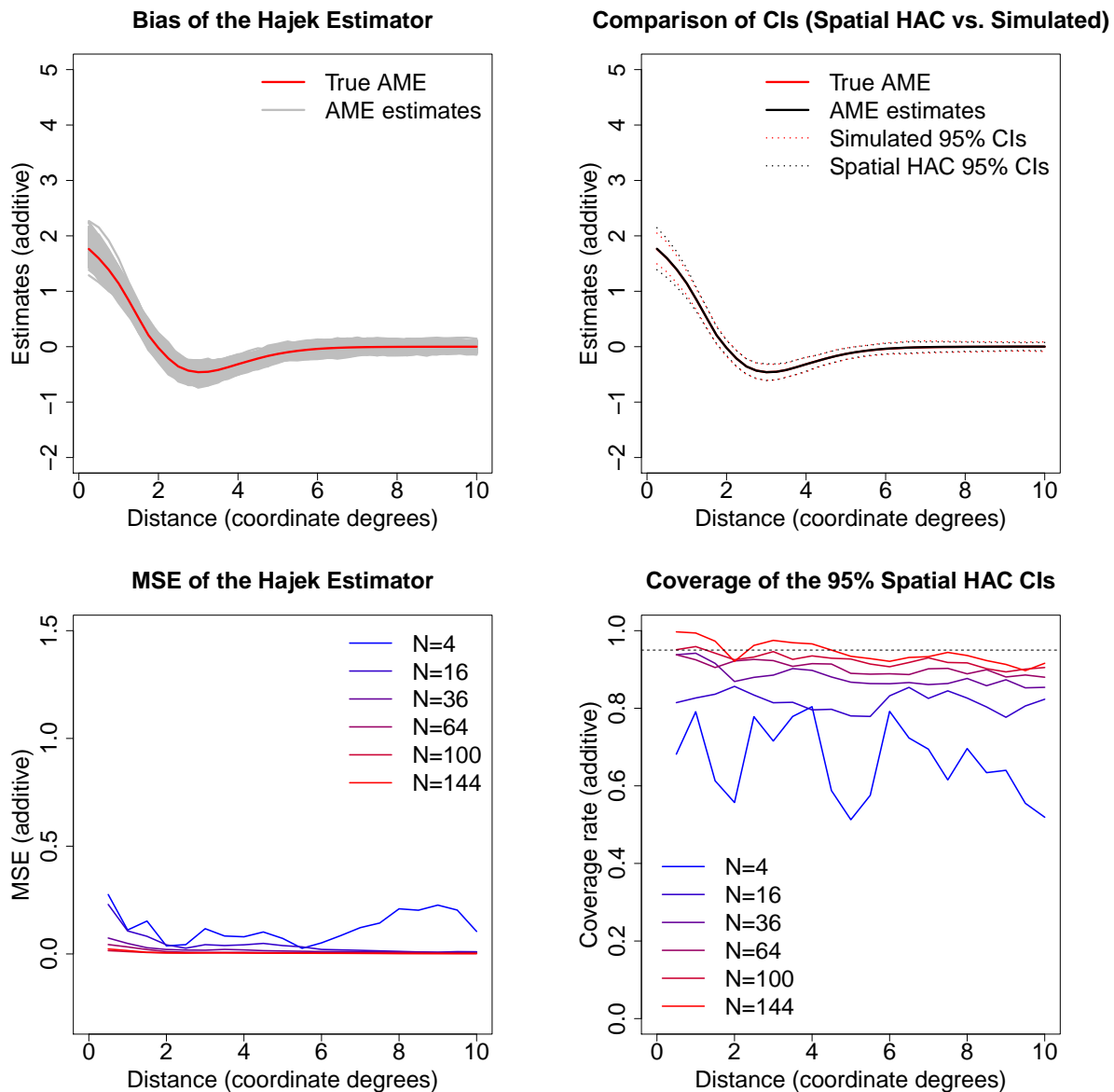


Figure 13: These plots show results from the Hajek estimator in the polygon intervention. The top-left plot presents the bias of the estimator. The top-right plot compares the simulated 95% confidence intervals with the averages of 95% Spatial HAC confidence intervals. The two plots on the bottom demonstrate how the MSE and the coverage rate of the estimator varies with sample sizes.

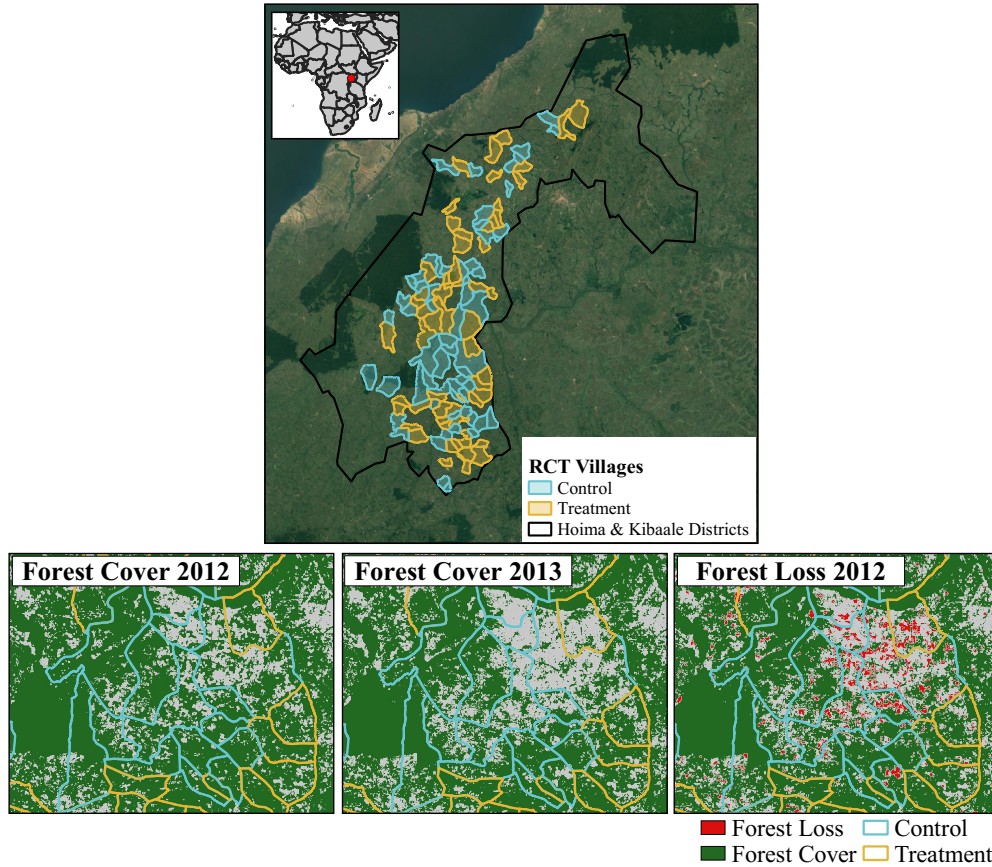


Figure 14: Top plot: The Global Forest Cover (GFC) dataset over a subset of the study area showing forest cover for 2012, 2013, and forest loss in 2012 (Hansen et al., 2013). Bottom plots: study area of randomized control trial for a PES program in Hoima and Kibaale district in Uganda, from Jayachandran et al. (2017). Boundaries of treatment (60) and control (61) villages were digitized using publicly available data and published maps.

B.3 Extra results from application

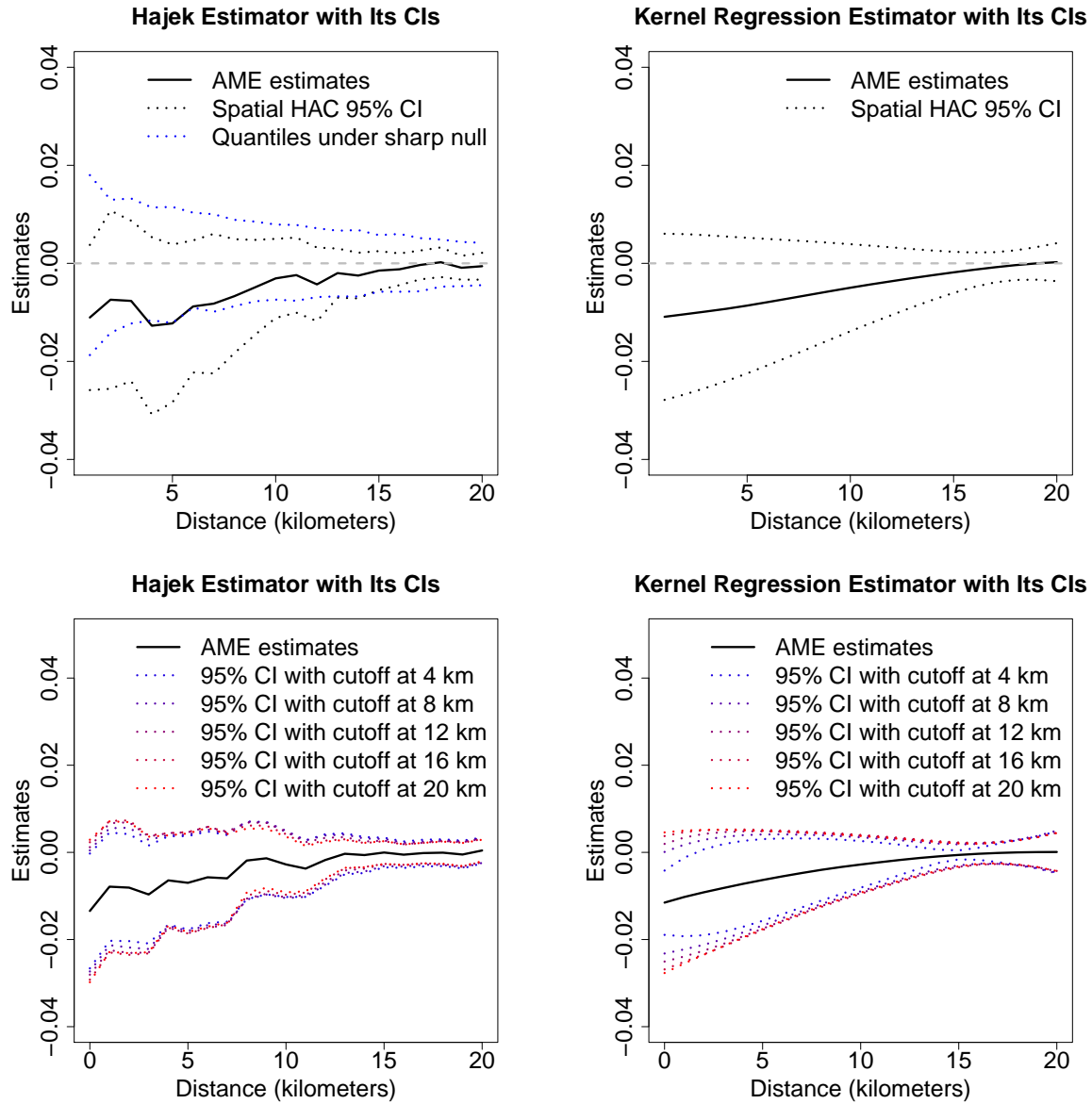


Figure 15: The plots on the top show results from the Hajek estimator (left) or the kernel regression estimator (right), when each village in the experiment is treated as a point rather than a polygon. We calculate distances from the geographic center of each village and calculate the circle averages across all the pixels on the edges of the circles. The black solid line represents the estimated AME at each distance value. The black dotted lines around it are the 95% spatial HAC confidence intervals. The blue dotted lines are the 2.5% and 97.5% quantiles of the effect estimates under sharp null. The plots on the bottom show how the 95% spatial HAC confidence intervals based on the Hajek estimator (left) or the kernel regression estimator (right) vary with the selected cutoff value. We consider five different choices, all the way from 4 km to 20 km.

References

- Arbia, G. (2006). *Spatial econometrics: statistical foundations and applications to regional convergence*. New York: Springer.
- Aronow, P. M. and C. Samii (2017). Estimating average causal effects under general interference, with application to a social network experiment. *Annals of Applied Statistics* 11(4), 1912–1947.
- Calonico, S., M. D. Cattaneo, and R. Titiunik (2014). Robust nonparametric confidence intervals for regression-discontinuity designs. *Econometrica* 82(6), 2295–2326.
- Conley, T. G. (1999). GMM estimation with cross sectional dependence. *Journal of Econometrics* 92, 1–45.
- Cox, D. R. (1958). *Planning of Experiments*. Wiley.
- Darmofal, D. (2015). *Spatial Analysis for the Social Sciences*. Cambridge: Cambridge University Press.
- Hainmueller, J., J. Mummolo, and Y. Xu (2019). How much should we trust estimates from multiplicative interaction models? simple tools to improve empirical practice. *Political Analysis* 27(2), 163–192.
- Halloran, M. E. and C. J. Struchiner (1995). Causal inference in infectious diseases. *Epidemiology*, 142–151.
- Hansen, M. C., P. V. Potapov, R. Moore, M. Hancher, S. A. Turubanova, A. Tyukavina, D. Thau, S. V. Stehman, S. J. Goetz, T. R. Loveland, et al. (2013). High-resolution global maps of 21st-century forest cover change. *science* 342(6160), 850–853.

- Hu, Y., S. Li, and S. Wager (2022). Average direct and indirect causal effects under interference. *Biometrika*.
- Hudgens, M. G. and M. E. Halloran (2008). Toward causal inference with interference. *Journal of the American Statistical Association* 103(482), 832–842.
- Imbens, G. W. and D. B. Rubin (2015). *Causal Inference for Statistics, Social, and Biomedical Sciences: An Introduction*. Cambridge: Cambridge University Press Press.
- Jayachandran, S., J. de Laat, E. F. Lambin, C. Y. Stanton, R. Audy, and N. E. Thomas (2017). Cash for carbon: A randomized trial of payments for ecosystem services to reduce deforestation. *Science* 357(6348), 267–273.
- Jenish, N. (2016). Spatial semiparametric model with endogenous regressors. *Econometric Theory* 32(3), 714–739.
- Jenish, N. and I. R. Prucha (2009). Central limit theorems and uniform laws of large numbers for arrays of random fields. *Journal of Econometrics* 150(1), 86–98.
- Kelejian, H. and G. Piras (2017). *Spatial Econometrics*. New York: Elsevier.
- Kojevnikov, D., V. Marmer, and K. Song (2021). Limit theorems for network dependent random variables. *Journal of Econometrics* 222(2), 882–908.
- Leung, M. P. (2022a). Causal inference under approximate neighborhood interference. *Econometrica* 90(1), 267–293.
- Leung, M. P. (2022b). Rate-optimal cluster-randomized designs for spatial interference. *The Annals of Statistics* 50(5), 3064–3087.
- Li, S. and S. Wager (2022). Random graph asymptotics for treatment effect estimation under network interference. *The Annals of Statistics* 50(4), 2334–2358.

- Miguel, E. and M. Kremer (2004). Worms: identifying impacts on education and health in the presence of treatment externalities. *Econometrica* 72(1), 159–217.
- Ogburn, E. L., O. Sofrygin, I. Diaz, and M. J. van der Laan (2020). Causal inference for social network data. *arXiv preprint arXiv:1705.08527*.
- Opsomer, J., Y. Wang, and Y. Yang (2001). Nonparametric regression with correlated errors. *Statistical Science*, 134–153.
- Papadogeorgou, G., K. Imai, J. Lyall, and F. Li (2020). Causal inference with spatio-temporal data: estimating the effects of airstrikes on insurgent violence in iraq. *arXiv preprint arXiv:2003.13555*.
- Raič, M. (2004). A multivariate clt for decomposable random vectors with finite second moments. *Journal of Theoretical Probability* 17(3), 573–603.
- Ross, N. et al. (2011). Fundamentals of Stein’s method. *Probability Surveys* 8, 210–293.
- Rubin, D. B. (2005). Causal inference using potential outcomes: Design, modeling, decisions. *Journal of the American Statistical Association* 100, 322–331.
- Samii, C. and P. M. Aronow (2012). On equivalencies between design-based and regression-based variance estimators for randomized experiments. *Statistics and Probability Letters* 82(2), 365–370.
- Särndal, C.-E., B. Swensson, and J. Wretman (1992). *Model Assisted Survey Sampling*. New York: Springer.
- Sävje, F., P. M. Aronow, and M. G. Hudgens (2021). Average treatment effects in the presence of unknown interference. *The Annals of Statistics* 49(2), 673–701.

- VanderWeele, T. J. and E. J. T. Tchetgen (2011). Effect partitioning under interference in two-stage randomized vaccine trials. *Statistics & probability letters* 81(7), 861–869.
- Wang, Y. (2021). Causal inference under temporal and spatial interference. *arXiv preprint arXiv:2106.15074*.
- Young, A. (2015). Improved, nearly exact, statistical inference with robust and clustered covariance matrices using effective degrees of freedom corrections. Unpublished Manuscript, London School of Economics.
- Zigler, C. M. and G. Papadogeorgou (2018). Bipartite causal inference with interference. *arXiv:1807.08660 [stat.ME]*.